AD-A194 486 EXPERIMENTAL INVESTIGATION OF THE EFFECTS OF UNDERWATER 1/1
EXPOSURE ON THE D.. (U) NAVAL POSTGRADUATE SCHOOL
MONTEREY CA R W DURHAM MAR 88

UNCLASSIFIED F/G 20/11 NL

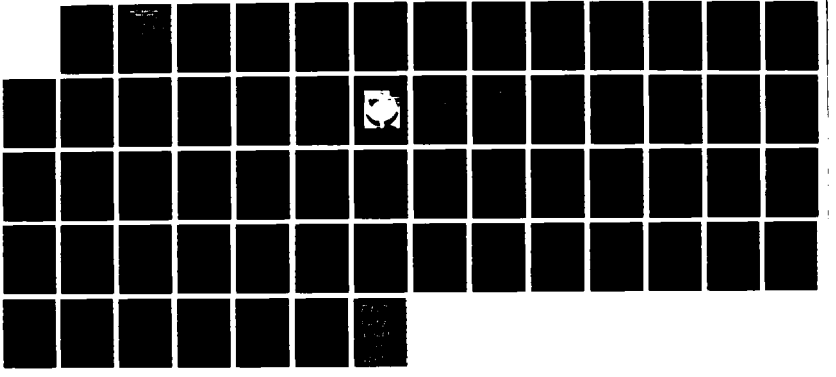

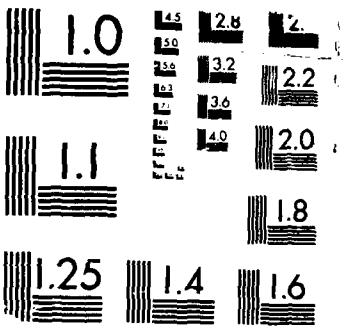

MICROCOPY RESOLUTION TEST CHART

BUREAU OF STANDARDS 1963-A

(2)

NAVAL POSTGRADUATE SCHOOL
Monterey, California

THESIS

EXPERIMENTAL INVESTIGATION OF THE EFFECTS OF UNDERWATER EXPOSURE ON THE DAMPING CHARACTERISTICS OF BOLTED STRUCTURAL CONNECTIONS FOR PLATES AND SHELLS

by

Richard W. Durham

March 1988

Thesis Advisor: Y. S. Shin

REPORT DOCUMENTATION PAGE

1a REPORT SECURITY CLASSIFICATION UNCLASSIFIED	1b RESTRICTIVE MARKINGS
2a SECURITY CLASSIFICATION AUTHORITY	3 DISTRIBUTION / AVAILABILITY OF REPORT Approved for public release; distribution is unlimited.
2b DECLASSIFICATION / DOWNGRADING SCHEDULE	
4 PERFORMING ORGANIZATION REPORT NUMBER(S)	5 MONITORING ORGANIZATION REPORT NUMBER(S)
6a NAME OF PERFORMING ORGANIZATION Naval Postgraduate School 6b OFFICE SYMBOL (If applicable) 69	7a NAME OF MONITORING ORGANIZATION Naval Postgraduate School
6c ADDRESS (City, State, and ZIP Code) Monterey, California 93943-5000	7b ADDRESS (City, State, and ZIP Code) Monterey, California 93943-5000
8a NAME OF FUNDING / SPONSORING ORGANIZATION 8b OFFICE SYMBOL (If applicable)	9 PROCUREMENT INSTRUMENT IDENTIFICATION NUMBER
8c ADDRESS (City, State, and ZIP Code)	10 SOURCE OF FUNDING NUMBERS PROGRAM ELEMENT NO. / PROJECT NO. / TASK NO. / WORK UNIT ACCESSION NO.

11 TITLE (Include Security Classification)
EXPERIMENTAL INVESTIGATION OF THE EFFECTS OF UNDERWATER EXPOSURE ON THE DAMPING CHARACTERISTICS OF BOLTED STRUCTURAL CONNECTIONS FOR PLATES AND SHELLS

12 PERSONAL AUTHOR(S)
Durham, Richard W.

13a TYPE OF REPORT	13b TIME COVERED	14 DATE OF REPORT (Year, Month, Day)	15 PAGE COUNT
Master's Thesis	FROM _____ TO _____	1988, March	

16 SUPPLEMENTARY NOTATION

17 COSATI CODES			18 SUBJECT TERMS (Continue on reverse if necessary and identify by block number)
FIELD	GROUP	SUB-GROUP	Viscous Fluid Damping, Underwater Excitation Shells and Plates, Structural Damping

19 ABSTRACT (Continue on reverse if necessary and identify by block number)

Recent studies have indicated that use of the bolted structural connection and the introduction of a viscoelastic material at the joint build-up can reduce the vibration response of a structure. Many potential applications utilizing this type of vibration reduction must operate in an underwater environment. A test structure consisting of two concentric circular shells connected by four vanes and assembled with bolts was tested to determine the effects of underwater exposure on the damping properties of a bolted structure. The effects of underwater exposure on system damping were examined for various structural bolt torques and for the application of a viscoelastic layer at the joint interfaces.

20 DISTRIBUTION / AVAILABILITY OF ABSTRACT	21 ABSTRACT SECURITY CLASSIFICATION	
☒ UNCLASSIFIED/UNLIMITED ☐ SAME AS RPT ☐ DTIC USERS	UNCLASSIFIED	
22a NAME OF RESPONSIBLE INDIVIDUAL Professor Young S. Shin	22b TELEPHONE (Include Area Code) (408) 646-2568	22c OFFICE SYMBOL 69SG

DD FORM 1473, 84 MAR — 83 APR edition may be used until exhausted. All other editions are obsolete

Block 19 cont.

With increasing underwater exposure time, the modal frequencies shifted forward and the frequency response amplitudes decreased. Modal damping was also noted to increase with underwater exposure time. After a finite period of underwater exposure time the system frequency responses stabilized and modal frequencies, damping and response amplitudes remained constant. The changes in the frequency response of the structure with underwater exposure resulted from the effects of increased viscous fluid layer damping at the joint interfaces. As water replaced the air at the joint interfaces, with continued underwater exposure, the effects of viscous fluid layer damping increased.

The introduction of water into the joint interfaces of a bolted joint generally increased the stiffness of the structure and resulted in increased structural damping. This effect was noted for the simple bolted case and to a smaller degree for the case with viscoelastic material at the joint interfaces.

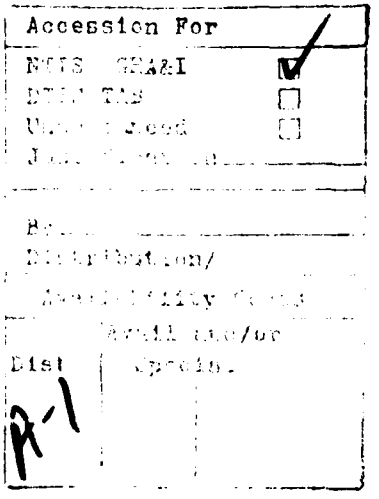

Approved for public release; distribution is unlimited.

Experimental Investigation of the Effects of Underwater Exposure on the Damping Characteristics of Bolted Structural Connections for Plates and Shells

by

Richard W. Durham
Lieutenant, United States Navy
B.S., University of Kansas, 1979

Submitted in partial fulfillment of the requirements for the degree of

MASTER OF SCIENCE IN MECHANICAL ENGINEERING

from the

NAVAL POSTGRADUATE SCHOOL

March 1988

Author: 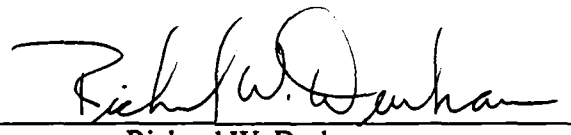
Richard W. Durham

Approved by: 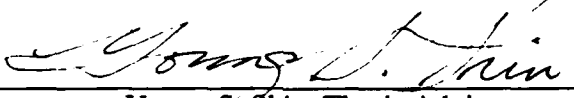
Young S. Shin, Thesis Advisor


Kilsoo S. Kim, Second Reader

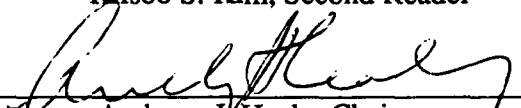
Anthony J. Healy, Chairman,
Department of Mechanical Engineering

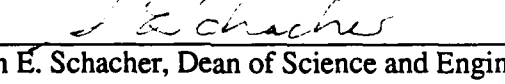
Gordon E. Schacher, Dean of Science and Engineering

ABSTRACT

Recent studies have indicated that use of the bolted structural connection and the introduction of a viscoelastic material at the joint build-up can reduce the vibration response of a structure. Many potential applications utilizing this type of vibration reduction must operate in an underwater environment. A test structure consisting of two concentric circular shells connected by four vanes and assembled with bolts was tested to determine the effects of underwater exposure on the damping properties of a bolted structure. The effects of underwater exposure on system damping were examined for various structural bolt torques and for the application of a viscoelastic layer at the joint interfaces.

With increasing underwater exposure time, the modal frequencies shifted forward and the frequency response amplitudes decreased. Modal damping was also noted to increase with underwater exposure time. After a finite period of underwater exposure time the system frequency responses stabilized and modal frequencies, damping and response amplitudes remained constant. The changes in the frequency response of the structure with underwater exposure resulted from the effects of increased viscous fluid layer damping at the joint interfaces. As water replaced the air at the joint interfaces, with continued underwater exposure, the effects of viscous fluid layer damping increased.

The introduction of water into the joint interfaces of a bolted joint generally increased the stiffness of the structure and resulted in increased structural damping. This effect was noted for the simple bolted case and to a smaller degree for the case with viscoelastic material at the joint interfaces.

TABLE OF CONTENTS

I. INTRODUCTION

A. BACKGROUND

Recently, attention has been given to improving structural damping by controlled interfacial slip in the joints of structures assembled with bolted fasteners [Refs. 1, 2]. Much of the inherent damping in a built-up structure originates in the these mechanical joints. The energy dissipation results from frictional forces due to small relative movements at the joint interfaces. This relative movement depends on the force or pressure holding the joint together. A low clamping force may result in the entire joint interface slipping, and is referred to as macroslip. Increased clamping forces may then result in regions of no slip and regions of very small slip, referred to as microslip. The controlling slip mechanism will depend on conditions at the joint and the magnitude of the applied excitation force. Joint damping may also be increased by the addition of an interfacial layer such as a polymer sheet [Ref. 3]. Iverson [Ref. 1] concluded that the reduction of bolt torque and the introduction of a viscoelastic material would increase the damping in a built-up structure of plates and shells. The increase in the inherent damping of a structure through improved joint damping design can reduce structural noise, dynamic response, stress, and fatigue. These improvements are very attractive in many naval applications.

B. PURPOSE

Many potential naval applications of vibration reduction through joint damping mechanisms would require the structure to operate in an underwater environment. The purpose of this study is to investigate the effects of underwater exposure on the joint damping mechanisms mentioned above. This will include the conditions of varied bolt torque and the addition of a viscoelastic layer at the joint interfaces. The effects on modal frequencies and damping and the changes in frequency response amplitudes will be studied for increasing underwater exposure times.

II. THEORY

A. MODAL ANALYSIS

A linear single degree of freedom system, subjected to a time varying input force with a corresponding time varying motion, can be described by a linear second order differential equation in the following form:

$$m\ddot{x}(t) + c\dot{x}(t) + kx(t) = f(t) \qquad 2.1$$

where,

$\ddot{x}(t)$ = acceleration response
$\dot{x}(t)$ = velocity response
$x(t)$ = displacement response
m = mass
c = damping
k = stiffness
$f(t)$ = applied force

A multiple degree of freedom system can be represented in a similar form:

$$M\ddot{x}(t) + C\dot{x}(t) + Kx(t) = F(t) \qquad 2.2$$

where,

$\ddot{x}(t)$ = acceleration response vector
$\dot{x}(t)$ = velocity response vector
$x(t)$ = displacement response vector
M = mass matrix, n x n
C = damping matrix, n x n
K = stiffness matrix, n x n
$F(t)$ = applied force vector

The mass, stiffness and damping matrices contain all the information required to determine the correct time response of a physical system. While the time domain behavior is important, frequency domain information may more clearly yield the desired information. The choice of the time or frequency domain is only a function of the desired information. [Ref. 4]

The Fast Fouier Transform (FFT) and the inverse FFT are utilized in digital signal processing to transfer data between the time and frequency domain. The discrete Fouier transform is the mathematical tool implemented on the digital signal analyzer to accomplish these transformations.Significantly, no information about the signal is lost or gained during the transformation from one domain to another. [Ref. 4]

The Laplace transform of Equation 2.1, the single degree of freedom system, is:

$$(ms^2 + cs + k)X(s) = F(s) \qquad 2.3$$

Solving for X(s) from the above equation gives:

$$X(s) = \frac{F(s)}{ms^2 + cs + k} \qquad 2.4$$

The polynomial in the denominator is called the characteristic equation, since the roots determine the nature of the time response. The roots of the characteristic equation are called the poles or singularities of the system. The roots of the numerator are called the zeros of the system. [Ref. 4]

A transfer function of a dynamic system is defined as the ratio of the output of the system to the system input, in the s-domain. The transfer function which relates the displacement to force is expressed as:

$$H(s) = \frac{X(s)}{F(s)} \qquad 2.5$$

Combining Equations 2.4 and 2.5, the transfer function is:

$$H(s) = \frac{1}{ms^2 + cs + k} \qquad 2.6$$

Since 's' is a complex variable, the transfer function has both a real and an imaginary part. The Fouier transform is obtained by substituting 'jw' for 's'. This special case of the transfer function is called the frequency response function and can be written as follows: [Ref. 4]

$$H(jw) = \frac{1/k}{1 + j2\zeta\frac{\omega}{\omega_n} - \frac{\omega^2}{\omega_n^2}} \qquad 2.7$$

$$\text{where, } \omega_n^2 = \frac{k}{m}, \ \zeta = \frac{c}{2\sqrt{km}}$$

The equations of motion for a more complex mechanical system with n-degrees of freedom, such as the one shown in Equation 2.2, may be written as:

$$B(s) \bullet X(s) = F(s) \qquad 2.8$$

where, F(s) = Laplace transform of the applied force vector
X(s) = Laplace transform of the resultant output vector
$B(s) = Ms^2 + Cs + K$
s = Laplace operator

B(s) is referred to as the system matrix. The transfer matrix, H(s), is defined as the inverse of the system matrix and satisfies the following equation:

$$X(s) = H(s) \bullet F(s) \qquad 2.9$$

Each element of the transfer matrix is a transfer function. [Ref. 4]

Modal analysis is defined as the study of the dynamic characteristics of a mechanical structure. The structural properties (damping, natural frequency, and modal frequency) can be determined from the system frequency response function curve fit representation generated by the digital signal analyzer. One fundamental assumption is that a mode of vibration can be excited at any point on the structure except at a node of vibration where there is no motion. As a result, the frequency and damping of any mode in a structure are constants and are called global properties of the structure. The mode shape amplitude at each point has a relative magnitude, depending on the excitation point, and is therefore called a local property. [Ref. 5]

B. VISCOELASTIC MATERIAL DAMPING

Viscoelastic damping is exhibited in many polymeric materials which are made up of long molecular chains. The carbon atoms join together strongly and can be branched so that the long chains can be strongly or weakly linked together. The damping arises from the relaxation and recovery of the polymer network after it has been deformed. There is strong dependence between material temperature effects and frequency effects because of the direct relationship between material temperature and molecular motion. [Ref. 6]

Temperature is usually considered to be the single most important environmental factor affecting the properties of damping materials. This effect is demonstrated in Figure 2.1. The storage modulus, E, is Young's modulus and the loss factor, η, is twice the damping factor. In the first region, the glassy region, the storage modulus is highest while the loss factor is very low. In the transition region, the storage modulus decreases rapidly while the loss factor reaches its highest value. Both the loss factor and storage modulus decrease slowly in the rubbery region.

In the fourth region the material softens and melts and is of little value in the design of damped systems. For most rubberlike materials the fourth region does not exist. [Ref. 6]

The most important effect of frequency is that the storage modulus always increases with increasing frequency. If a large frequency range, such as 10 decades, is of interest, the variation of damping properties with frequency at a fixed temperature is illustrated in Figure 2.2. [Ref. 6]

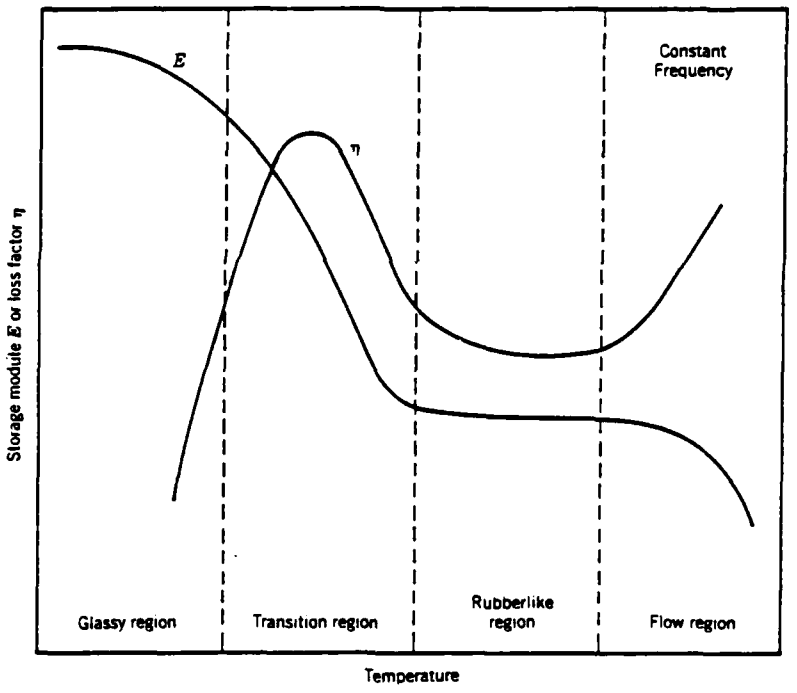

Figure 2.1. Variation of the storage modulus and loss factor with temperature. [Ref. 6]

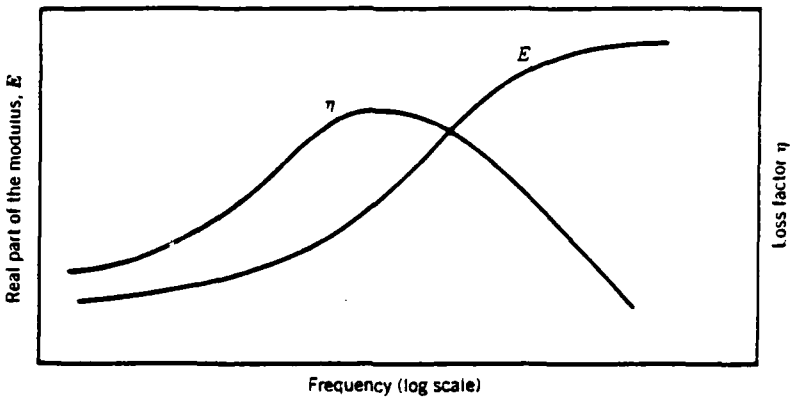

Figure 2.2. Variation of storage modulus and loss factor with frequency. [Ref. 6]

Other variables affect the storage modulus and loss factor and can be important under certain circumstances. The variation of damping properties with dynamic strain is similar to that of temperature, but the effect is much smaller. Static preload affects the dynamic properties of material and is most important in the rubbery region. The storage modulus increases with increasing static preload while the loss factor decreases. The damping properties of rubberlike materials are often affected by environmental factors such as aging, oil, salt water, vacuum and pressure. Adverse conditions and the protection of the damping material must be considered in the design of damped systems. [Ref. 6]

Constrained layer damping treatments are an efficient method of designing damping into a structure. A single constrained layer consists of a thin layer of damping material applied to a base structure and then backed with a constraining layer as shown in Figure 2.3.

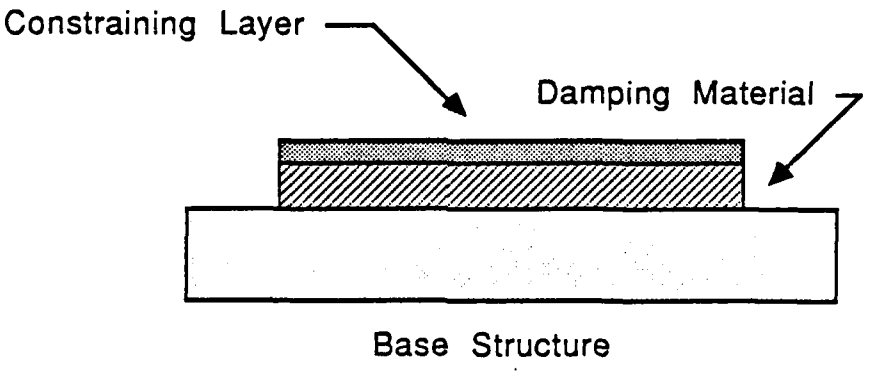

Figure 2.3. Single constrained layer arrangement.

The damping mechanism in this configuration is cyclic shear deformation of the damped layer. In analyzing constrained layer treatments, it is usually appropriate to neglect bending deformations and assume all deformations in the damping material to be shear. With this in mind, for the case of linear viscoelastic material, the energy dissipated by the material is given by:

$$D_s = \pi \int_{vol} \eta E \gamma^2 dv \qquad 2.10$$

Significantly, the energy loss represented by Equation 2.10 is dependent on two types of terms. The 'ηE' term (loss modulus) is a property of the damping material while the 'γ^2' term (shear loss) is a measure of dynamic strain which is a function of the geometry of the damping treatment. [Ref. 6] Thus, optimization of a damping treatment depends not only on the proper choice of a damping material, but on the positioning of the treatment with respect to the modal characteristics of the structure to be damped. The placement of a constrained layer on a portion of a structure not undergoing major motion would be ineffective. [Ref. 6]

Viscoelastic damping design is even more complicated than choosing the proper material and location. It has been shown that constrained layer treatments have an inherent frequency, or more precisely, a wave length dependency. For a given viscoelastic material, constraining layer, frequency range, and temperature there is an optimum constraining layer length. [Ref. 6]

A more detailed discussion of this and other considerations can be found in Reference six.

C. VISCOUS FLUID LAYER DAMPING

Two plates in close contact with each other have a marked improvement in vibrational damping rate and the attenuation of radiated noise. Viscous losses in the fluid layer between the two plates are in part responsible for these improvements. [Ref. 7]

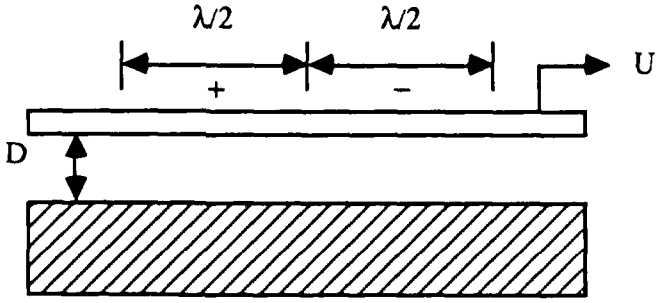

Figure 2.4. Damping mechanism due to viscous fluid layer damping.

Consider the plate arrangement shown in Figure 2.4. The plate is driven by a harmonic pressure distribution with a wave length, λ and an angular frequency, ω. It is backed by a rigid plane structure a distance 'D' from the plate with a viscous fluid in the channel between the wall and the plate. As shown in Figure 2.4 ,there are two adjacent regions of the plate which are half-a-wave-length in length and are designated positive, +, and negative, −. As the plate moves, the fluid is pumped from the positive region to the negative region. The viscous shear stresses at the wall correspond to a pressure drop between the positive and negative regions. Under such conditions, the contributions to the pressure change in the fluid below the positive region will act as a friction force per unit area. Ingard and Akay [Ref. 7] go on to develop the following relationship for the system damping factor:

$$\eta \approx \frac{\mu\lambda^2}{\omega_0 m D^3} \qquad 2.11$$

where,
μ = coefficient of viscosity
λ = harmonic wave length
m = mass of plate
D = fluid layer thickness
ω_0 = resonant frequency
η = loss factor

Note that this relationship predicts that the damping factor of a viscous fluid between two plates will increase with increasing fluid viscosity. [Ref. 7]

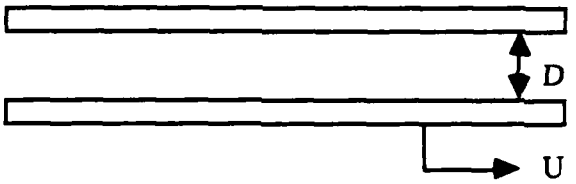

Figure 2.5. Two plates separated by a viscous fluid layer.

Additionally, Akay and Ingard [Ref. 7] developed the following relationship concerning the resonant frequency for a two plate system as shown in Figure 2.5, undergoing forced harmonic motion:

$$\omega_0 = \sqrt{\frac{\rho_l c_l}{m\, D \cos^2\phi}} \qquad 2.12$$

where, ρ_1 = fluid density

c_1 = speed of sound in fluid layer

U = phase velocity of input force

$\phi = \sin^{-1} \frac{U}{c_1}$

Note that this relationship predicts that the resonant frequency of a plate system such as that in Figure 2.5 will increase as the square root of fluid density and the speed of sound in the medium between the plates increases.

III. EXPERIMENTAL METHOD

A. EXPERIMENTAL MODEL

The experimental model was the same model used by Iverson [Ref. 1] in his investigation of damping characteristics of a bolted structure. The model consisted of two concentric shells connected by four vanes. The outer shell was rolled and welded, and the vane connections were welded, while all other connections were made with bolts as shown in Figure 3.1. The outer rolled shell was constructed of 0.25 inch carbon steel , the vanes were 0.25 inch bronze, and the inner shell was 0.50 inch bronze. High strength bolts with a diameter of 0.75 inches and double washers were used in assembling the structure. The model was supported with shock cord to limit the transmission of random noise from the environment to the structure.

During the second phase of the investigation 3M ISD-112 viscoelastic material with a thickness of 20 mil was applied to the joint interfaces. This damping material was chosen because of its consistent loss factor over a wide range of temperatures. The nomograph, demonstrating the performance of the ISD-112 at various frequencies and temperatures, is included as Figure 3.2.

Maximum contact force calculations were determined using typical machine design calculations:

$$Fi = 0.9 \times Sp \times At$$

where 'Fi' was the proof load, 'Sp' the proof strength of the bolt material, and 'At 'the tensile-stress area. The result was then used to obtain the bolt torque as follows:

$$T \cong 0.2 \times Fi \times D$$

where 'T' was the bolt torque and 'D' the bolt diameter . The maximum bolt torque was determined to be 320.0 ft-lb and the maximum contact force to be 3.06×10^6 lb. For consistency with Iverson, all references to bolt torque and contact force will be listed in percentages of these maximum values. [Ref. 1]

B. MODAL TESTING ARRANGEMENT

The testing equipment arrangement used during investigation is shown in Figure 3.3. The input force was provided by a Wilcoxon Research F7/F4 Vibration Generator mounted vertically on the right vane (looking at the structure), 12 inches from the front and 4 inches

outboard of the inner shell. The vibration generator was encased in a water-tight plexiglass container to allow for underwater excitation of the structure. The vibration generator combined both an electromechanical and a piezoelectric unit to provide a variable power output for the range of 10 to 15,000 Hz. A Wilcoxon Power Amplifier provided the driving power which was split into two signals by a Wilcoxon Matching Network to power both units of the vibration generator. An HP-3562A Dynamic Signal Analyzer provided the control signal to the power amplifier. A force transducer was mounted at the base of the vibration generator and was used to measure the input excitation force. This force input signal was amplified by a charge amplifier and fed to channel one of the HP-3562A Dynamic Signal Analyzer.

Two Endevco accelerometers were permanently mounted on the structure to measure its response, as shown in Figures 3.1 and 3.2. One accelerometer was mounted on the shell, 12 inches above the right vane and four inches from the front of the structure. The other accelerometer was mounted on the right vane, eight inches outboard of the inner shell and four inches from the front of the structure. The outputs of these accelerometers were fed through signal conditioners and were used to measure the response of the structure. These outputs were fed, one at a time, to channel two of the HP-3562A Dynamic Signal Analyzer.

All structural measurements were performed with the HP-3562A Dynamic Signal Analyzer using a swept sine control signal, with ten averages at each data point. The selection of ten averages was based on providing a good coherence estimate for all measurements. The HP 3562A sampled, digitized and filtered the analog input signals. This was done because the Fast Fouier Transform algorithm required digital inputs to transform time domain data to the frequency domain. With this data, the analyzer calculated the frequency response, power spectrums, and coherence function. These measurements were displayed, analyzed and saved for further comparison.

C. TESTING PROCEDURE

1. Case Without Viscoelastic Material

The first phase of testing was performed without viscoelastic material at the joint interfaces. The model was disassembled, dried and reassembled with a 10 percent bolt torque applied to each bolt. Baseline (dry) frequency response measurements were performed in air over six frequency ranges: 15 to 115 Hz, 100 to 200 Hz, 200 to 300 Hz, 95 to 115 Hz, 120 to 140 Hz, and 220 to 270 Hz. The model was then immersed in water and agitated over a frequency range of 15 to 1015 Hz with the vibration generator for two hours. It was then lifted out of the water,the surfaces of the model were dried, and

frequency response measurements were performed over the same six frequency ranges listed above, and compared to the baseline measurements. The model was then immersed in water and agitated for four more hours, lifted out, dried, and again frequency response measurements were performed and compared to the baseline measurements. This sequence was repeated two more times with the model having a total of 14 hours of underwater agitation prior to the last set of frequency response measurements being taken .
The entire procedure listed above was repeated for 20 percent bolt torque and again for 40 percent bolt torque.

2. Case With Viscoelastic Material

The second phase of testing was performed with viscoelastic material at the joint interfaces. The model was disassembled, dried and reassembled with viscoelastic material at the joint interfaces and a bolt torque of 40 percent. The same procedure listed above of obtaining baseline data and repeated underwater agitation followed by frequency response measurements was performed for 40 percent bolt torque. Bolt torque was then reduced to 20 percent, the structure was agitated underwater for eight hours, removed from the water and frequency response measured over the six frequency ranges listed above. Bolt torque was reduced to 10 percent, and again the structure was agitated underwater for eight hours, removed from the water and frequency response measured.

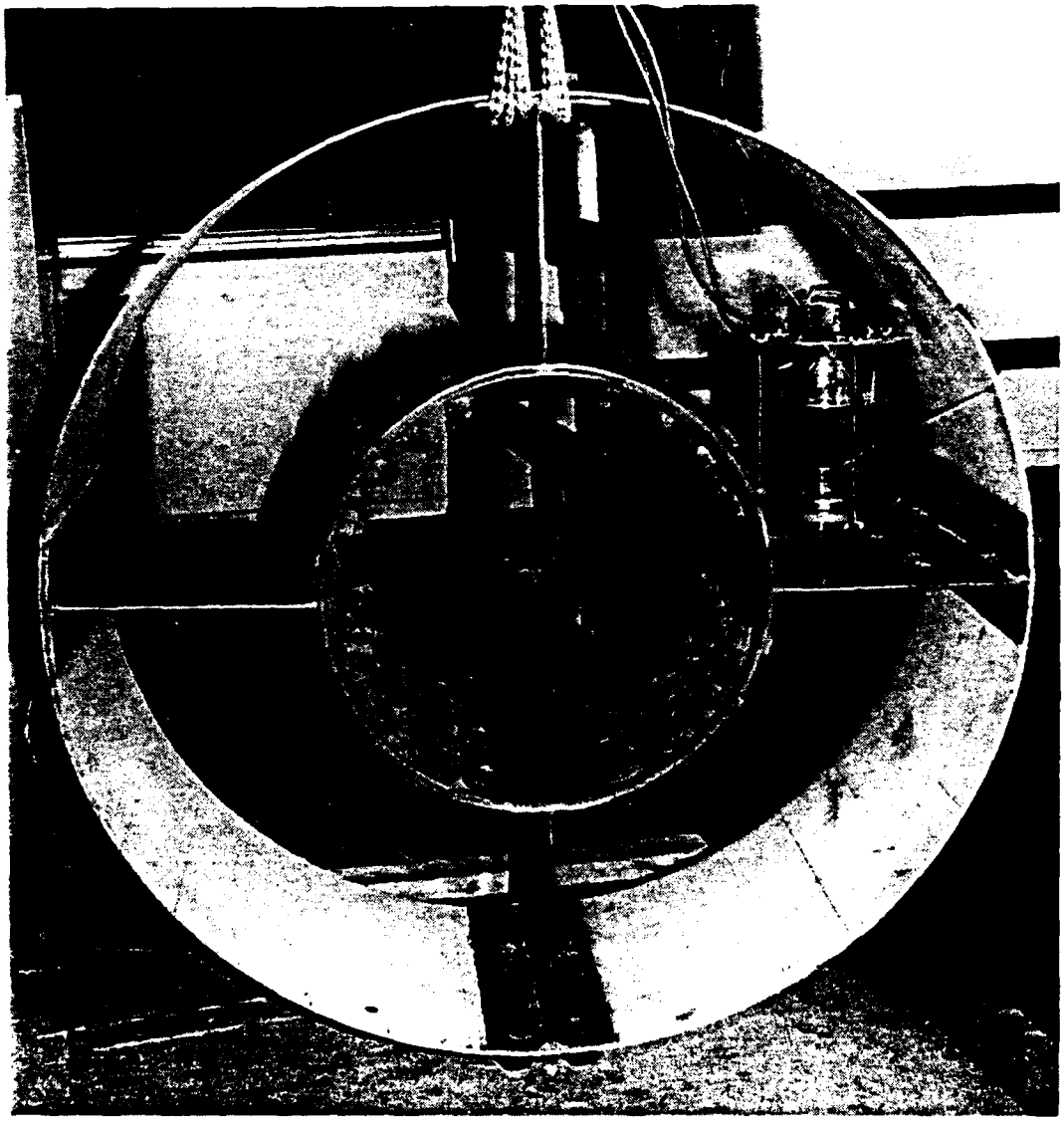

Figure 3.1. The test model.

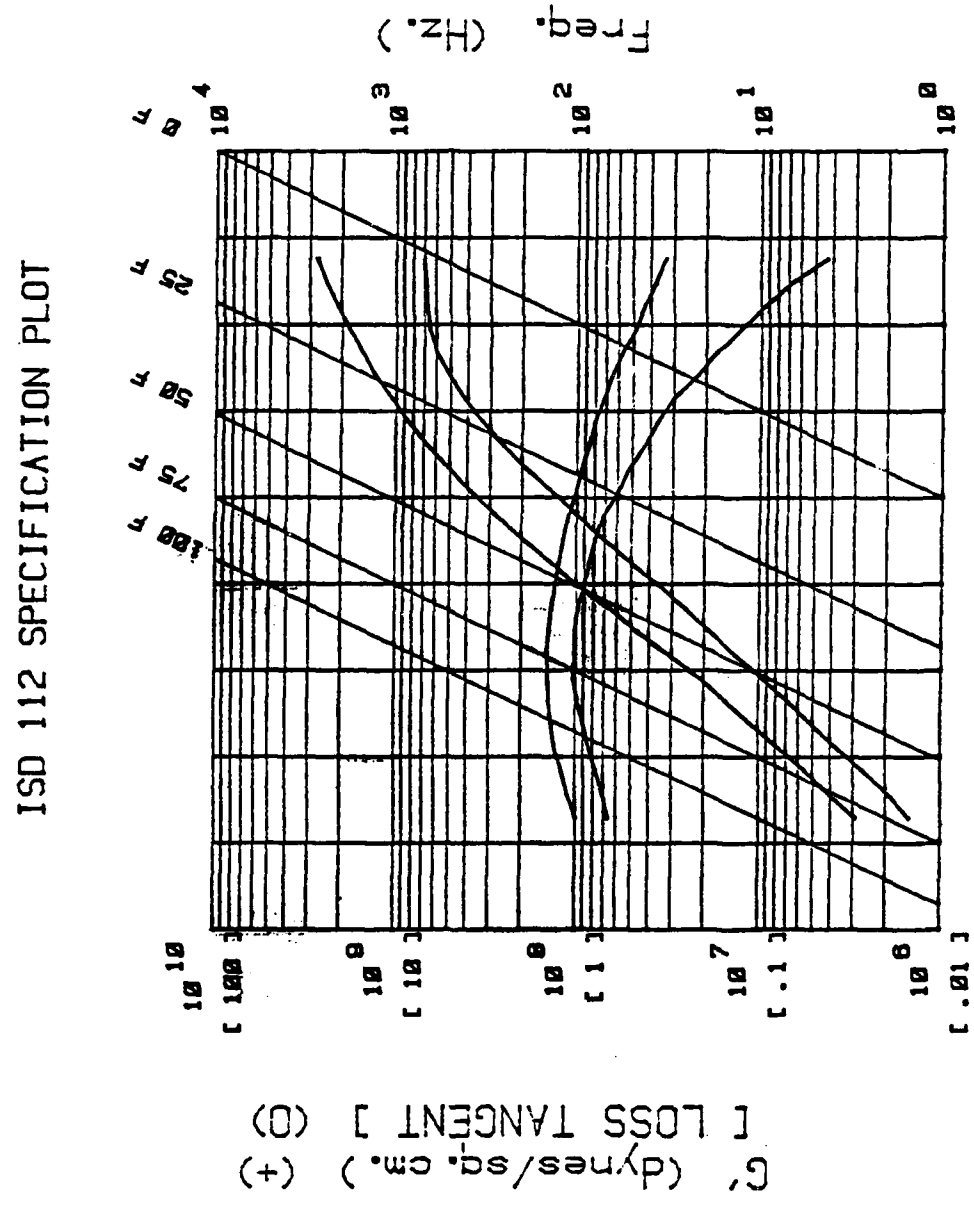

Figure 3.2. ISD-112 viscoelastic material nomograph.

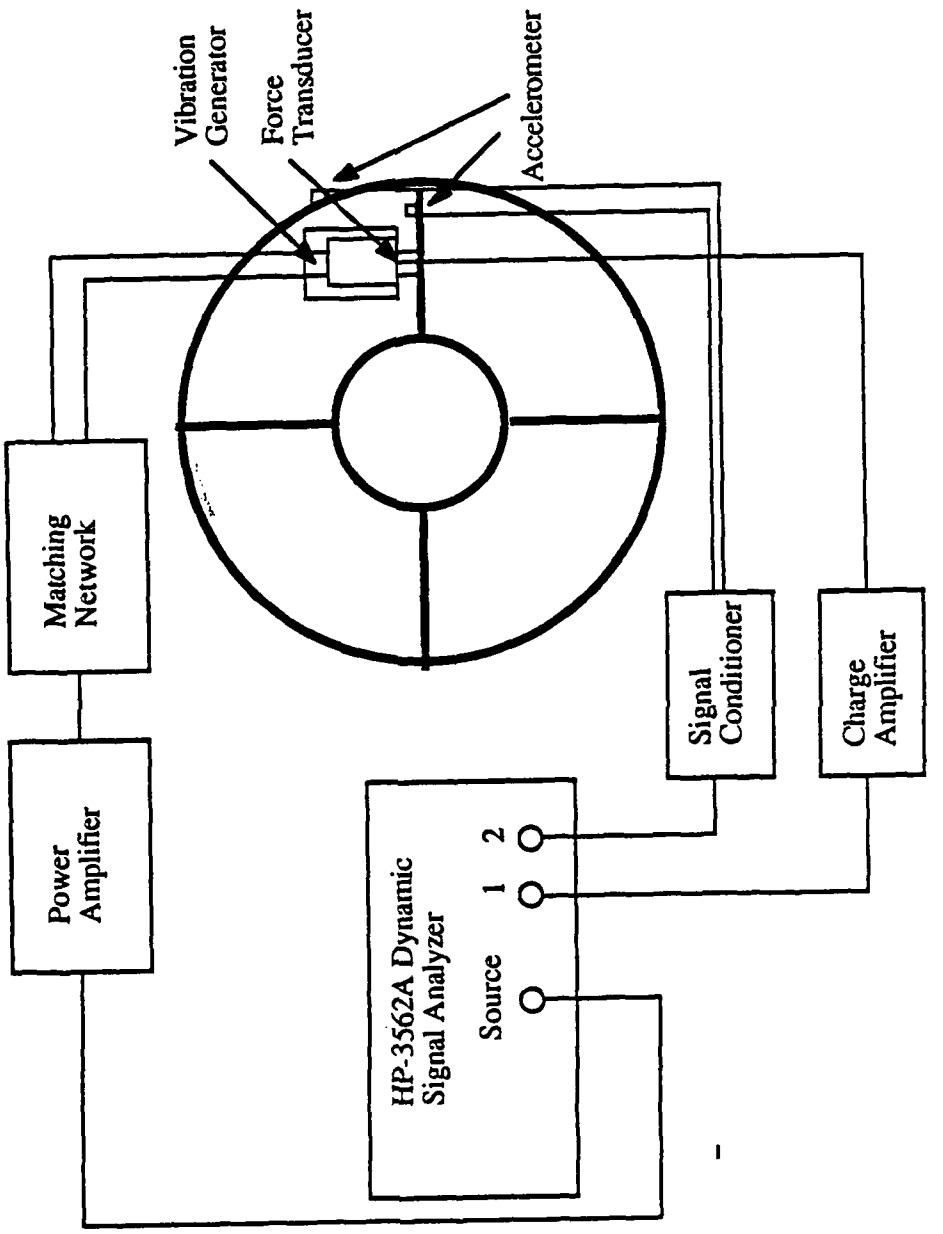

Figure 3.3. Test equipment arrangement.

IV. RESULTS

A. CASE WITHOUT VISCOELASTIC MATERIAL AT JOINT INTERFACES

The frequency response functions of the shell for the 15 to 115 Hz range with 14 hours of underwater agitation and 40 percent bolt torque, without viscoelastic material at the joint interfaces, are shown in Figure 4.1. The solid lines represent the frequency response when dry (baseline) while the dashed lines represent the frequency response after the underwater agitation. Frequency shifts, upward in nature from the baseline, are clearly visible at the modes corresponding to 43, 55, and 87 Hz . There were no other clearly noticeable shifts at the other modal frequencies within this range. The frequency response amplitudes decreased from the baseline measurements at nearly all the modes in this range. The frequency response functions for the 100 to 200 Hz range, under the same conditions as those above, are shown in Figure 4.2. Upward frequency shifts are clearly noticeable at all modal frequencies except for those at 100 and 102 Hz. The frequency response amplitudes decreased at all modes in this range. The frequency response functions for the 200 to 300 range, again for the conditions listed above, are shown in Figure 4.3. In this range, all modal frequencies shifted up in frequency and all frequency response amplitudes decreased when compared to the baseline. Significantly, the amplitudes at the modes associated with 217, 255, and 265 Hz decreased by approximately 10 dB below the baseline.

In order to obtain a higher resolution in certain areas of interest, three measurements were taken over narrower frequency spans for the same conditions as listed above. The frequency response function for the 95 to 115 Hz range is shown in Figure 4.4. Upward frequency shifts at the modes associated with 100 and 100.1 Hz that were not noticeable in the wider frequency span measurements of Figure 4.1 became noticeable. The frequency response function for the 120 to 140 Hz range is shown in Figure 4.5. The two modes at 127 and 127.5 Hz shown in this figure were shown as a single mode in the wider frequency span measurements of Figure 4.2. The frequency response functions for the 230 to 270 Hz range are shown in Figure 4.6. An upward frequency shift from the baseline measurements is clearly noticeable throughout this range. A measured reduction of 12 dB below the baseline was obtained at the 267 Hz mode. Also, the change in mode response shape is an indication of the increased damping at this mode.

The frequency response functions for the 10 and 20 percent bolt torque conditions showed similar changes, after the underwater agitation, as compared to the response functions for the 40 percent condition. For example, the frequency response functions for 20 percent bolt torque, measured at the shell, with 14 hours underwater agitation for the

frequency spans of 95 to 115 Hz, 120 to 140 Hz and 230 to 270 Hz are shown in Figures 4.7, 4.8, 4.9. However, in Figure 4.7, the amplitude increases at the 100 Hz mode after the underwater agitation. This also happens at the 240 Hz mode shown in Figure 4.9.

The frequency response functions measured from the accelerometer positioned on the vane showed the same characteristics as the those discussed above for the shell. For example, the frequency response functions for 10 percent bolt torque, measured at the vane, with 14 hours of underwater agitation for the frequency spans of 95 to 115 Hz, 120 to 140 Hz and 230 to 270 Hz are shown in Figures 4.10, 4.11, 4.12.

In Figure 4.13, the 20 and 40 percent bolt torque conditions are compared for the 95 to 115 Hz frequency range, measured at the shell, after two hours of underwater agitation. With reduced bolt torque the the frequency response function clearly shifts to the left, consistent with Iverson's [Ref. 1] results for reduced bolt torque in the dry condition. This downward shift in frequency response continues when the 10 and 40 percent bolt torque conditions for the same range and underwater agitation time are compared in Figure 4.14. These comparisons are seen again for the 120 to 140 Hz ranges in Figures 4.15 and 4.16 for two hours of underwater agitation, with the same results. Additionally, a decrease in modal amplitude accompanied the downward frequency shifts when bolt torque was reduced.

The upward shift in frequency response was a function of the underwater agitation time of the structure. With increased underwater agitation, the modal frequencies continued to shift upward until the total accumulated underwater agitation time was approximately 14 hours. After 14 hours of accumulated underwater agitation there were only minor changes in the frequency response functions with additional underwater agitation time.

B. CASE WITH VISCOELASTIC MATERIAL AT JOINT INTERFACES

The corresponding frequency response functions over the same six ranges of interest, for the 40 percent bolt torque condition,14 hours of underwater agitation, and viscoelastic material at the shell/vane joint interfaces, are shown in Figures 4.17 through 4.22. Again, the same general upward shift in frequency and decrease in response amplitude from the baseline conditions are noted. The frequency shifts and amplitude decreases, from the dry (baseline) measurements, are generally less than those for the structure without the addition of viscoelastic material.

In Figure 4.23, the 40 percent bolt torque conditions with and without viscoelastic material after two hours of underwater agitation are compared for the 95 to 115 Hz range. This comparison is made again for the 120 to 140 Hz range in Figure 4.24. The cases with viscoelastic material show a clear downward shift in frequency at the resonance peaks and a

decrease in the modal amplitudes. This is consistent with the relative frequency shifts observed in the dry state when viscoelastic material is applied.

The 20 percent bolt torque condition with and without viscoelastic material, after maximum underwater agitation, is compared for the 95 to 115 Hz and 120 to 140 Hz ranges in Figures 4.25 and 4.26. In Figures 4.27 and 4.28 the 10 percent bolt torque condition with and without viscoelastic material are compared for the same ranges listed above. The frequency shift is again to the left and the modal amplitudes decrease with the addition of viscoelastic material for both bolt torques.

C. STRUCTURAL DAMPING

Structural damping was calculated for some of the modal peaks in the narrow frequency range measurements. This was done using the half-power method after a localized curve fit of each resonance peak of interest. The percent damping for 40 percent with viscoelastic material, 40 percent without viscoelastic material, 20 percent and 10 percent bolt torques verses frequency are graphed in Figures 4.29 through 4.32 respectively. Both the dry (baseline) and the condition with 14 hours of underwater agitation are graphed. In Figure 4.29, 40 percent bolt torque with viscoelastic material, the damping increased with underwater agitation, but the increase is not as significant as the increase for the 40 percent bolt torque with no viscoelastic material. As the bolt torque was decreased, the percent damping increased,both dry and after agitation, as shown by comparing Figures 4.30, 4.31, and 4.32. The structural damping was below one percent in all cases with the highest damping measured for the case with viscoelastic material at the joint interfaces. In all cases, percent damping was noted to increase following the underwater agitation.

D. DISCUSSION

With increasing underwater agitation, the water gradually replaced the air between the bolt flanges at the joint interfaces of the model. Equation 2.11 predicts that the viscous damping will increase for a simple two plate structure as the viscosity of the medium between the plates increases. Although the shell and plate structure studied is considerably more complex, the increase in system damping results from the increased contribution of the viscous damping as the water displaces the air at the joint interfaces. Equation 2.11 also predicts that viscous damping will decrease as the distance separating the plates increases. This effect can be noted by comparing the increases in system damping with underwater exposure for 40 and 20 percent bolt torque conditions in Figures 4.29 and 4.31. With decreased bolt torque, the force holding the flange plates together at the joint

interfaces of the model decreases and the distance between the flange plates increases. The relative increase in system damping with underwater agitation is less for the 20 percent bolt torque case than for the 40 percent case as shown in Figures 4.29 and 4.31, consistent with the predictions of Equation 2.11.

Equation 2.12 predicts that the natural frequencies of a simple two plate system will increase with the increase in density and sonic speed of the fluid separating the plates. This increase in the natural frequencies with increasing underwater agitation was noted throughout the study of the more complicated shell and plate model.

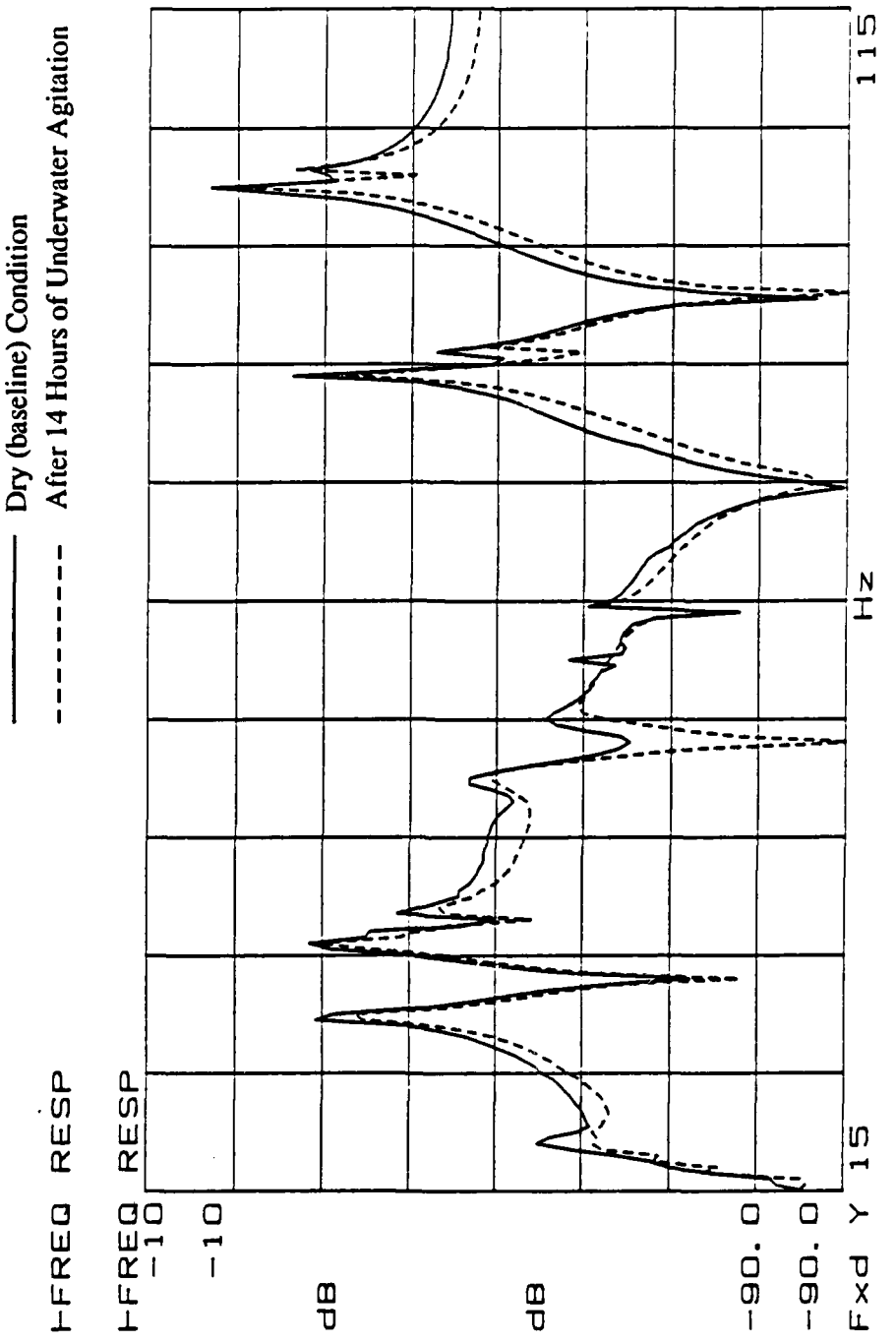

Figure 4.1. Frequency response of structure, measured on the shell, at 40 % bolt torque with no viscoelastic material. Solid line represents the baseline condition and the dashed line represents the structure after 14 hours of underwater agitation.

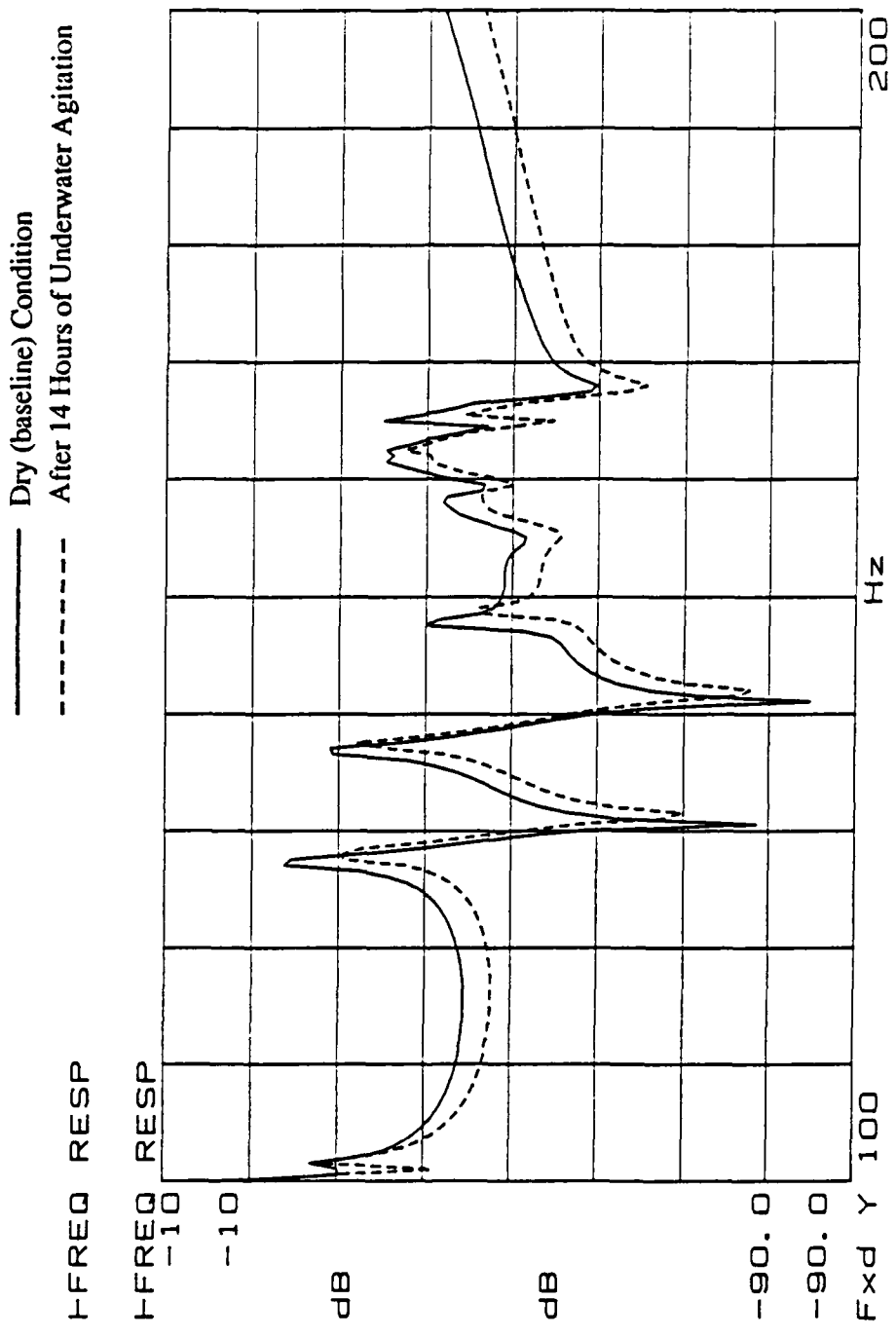

Figure 4.2. Frequency response of structure, measured on the shell, at 40 % bolt torque with no viscoelastic material. Solid line represents the baseline condition and the dashed line represents the structure after 14 hours of underwater agitation.

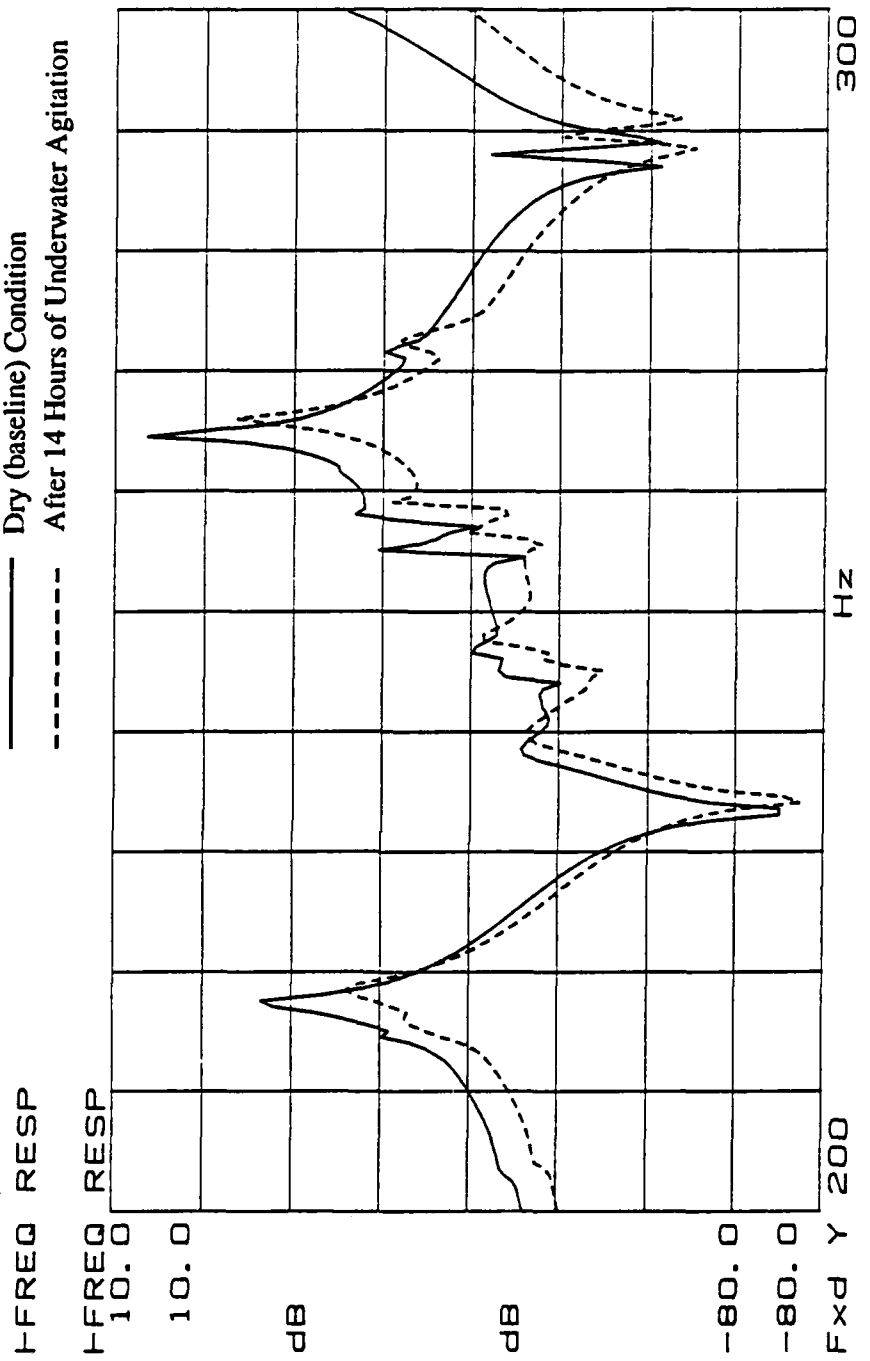

Figure 4.3. Frequency response of structure, measured on the shell, at 40 % bolt torque with no viscoelastic material. Solid line represents the baseline condition and the dashed line represents the structure after 14 hours of underwater agitation.

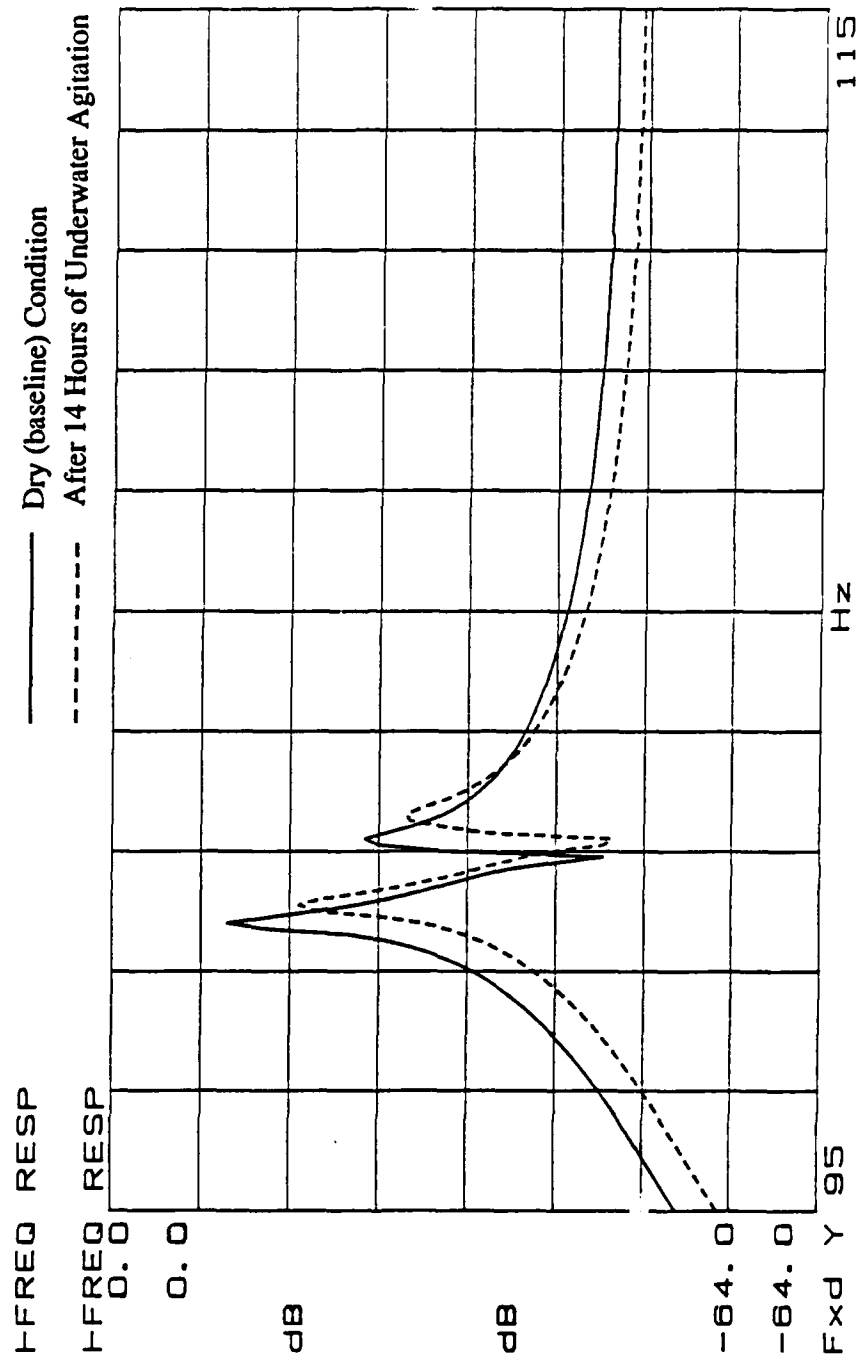

Figure 4.4. Frequency response of structure, measured on the shell, at 40 % bolt torque with no viscoelastic material. Solid line represents the baseline condition and the dashed line represents the structure after 14 hours of underwater agitation.

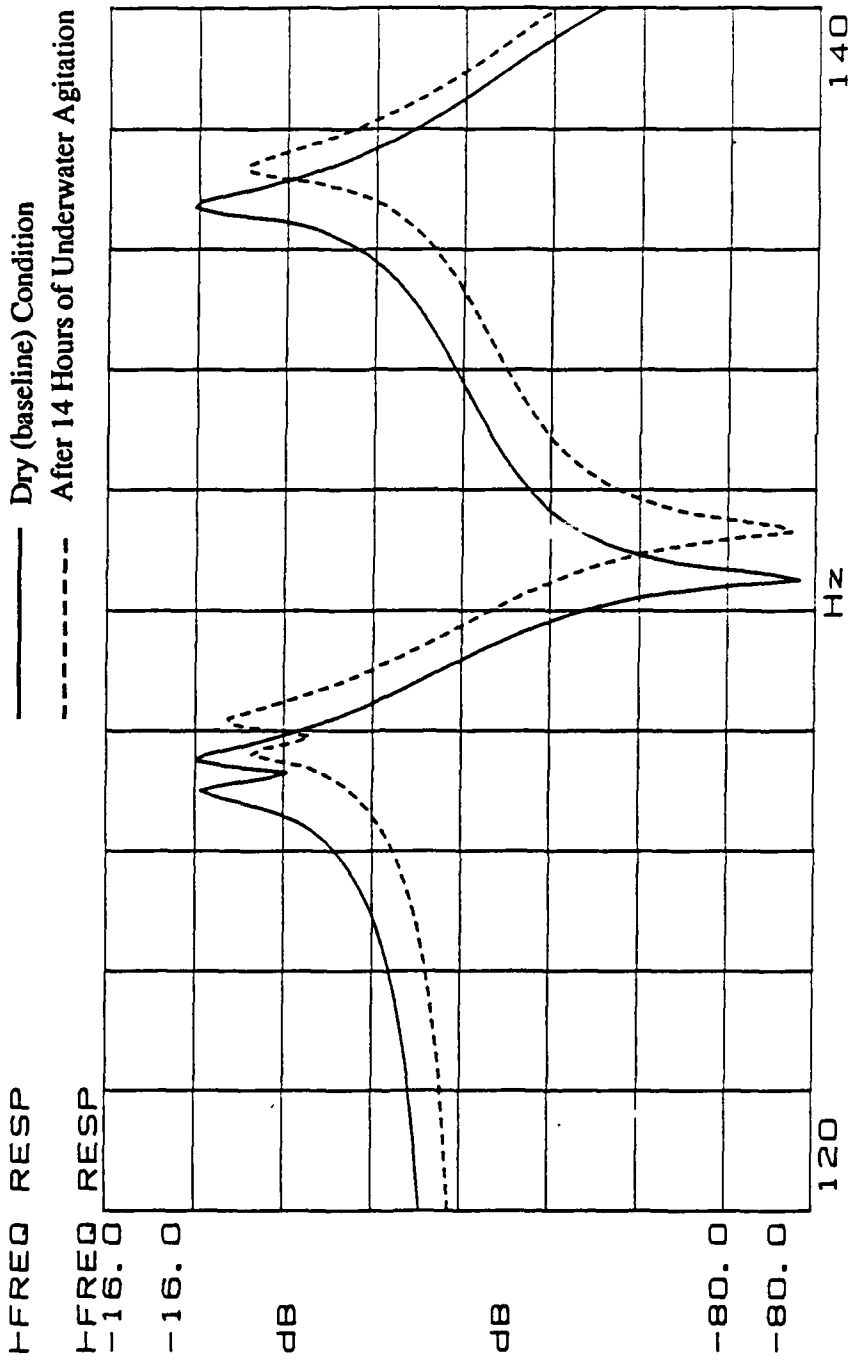

Figure 4.5. Frequency response of structure, measured on the shell, at 40 % bolt torque with no viscoelastic material. Solid line represents the baseline condition and the dashed line represents the structure after 14 hours of underwater agitation.

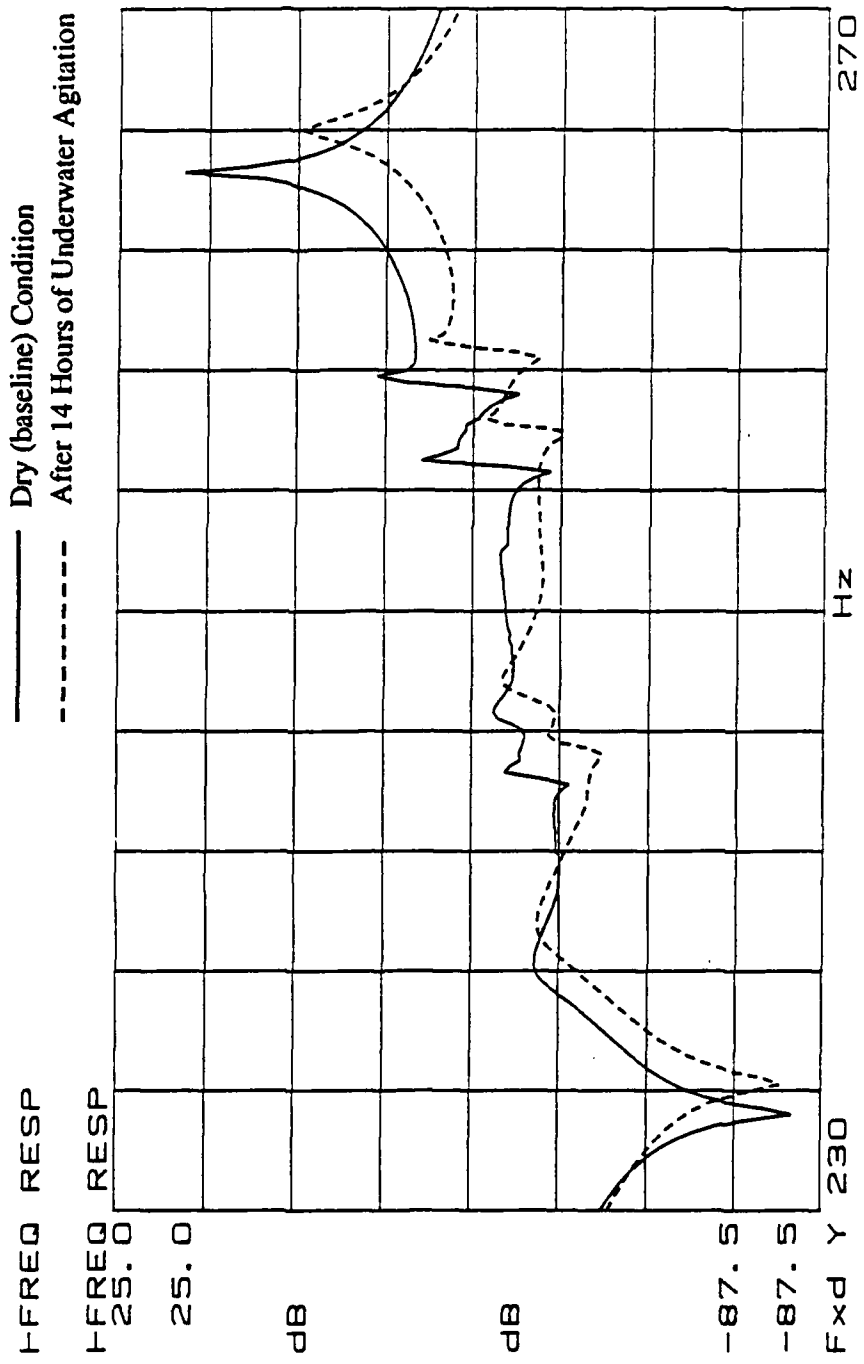

Figure 4.6. Frequency response of structure, measured on the shell, at 40 % bolt torque with no viscoelastic material. Solid line represents the baseline condition and the dashed line represents the structure after 14 hours of underwater agitation.

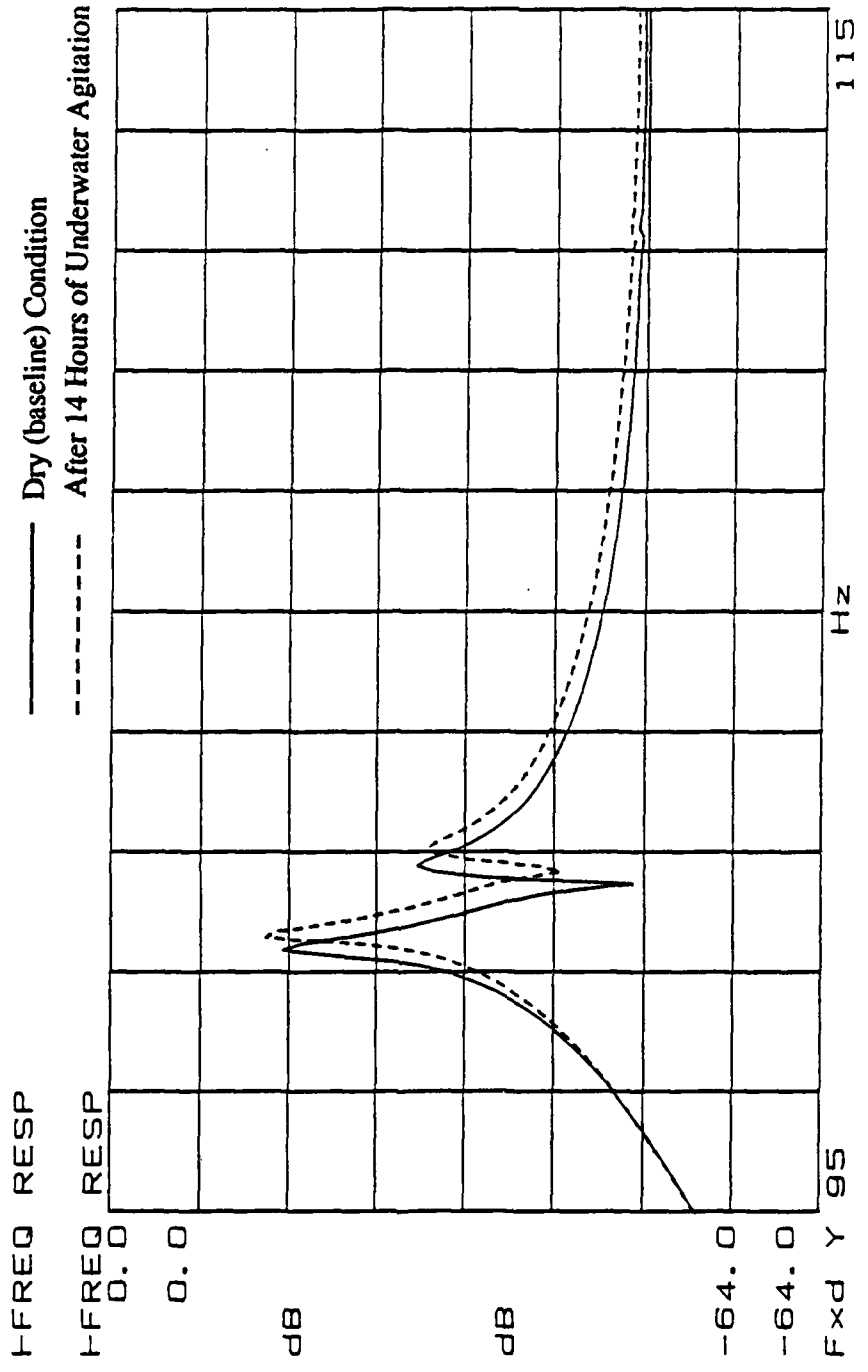

Figure 4.7. Frequency response of structure, measured on the shell, at 20 % bolt torque without viscoelastic material. Solid line represents the baseline condition and dashed line represents structure after 14 hours of underwater agitation.

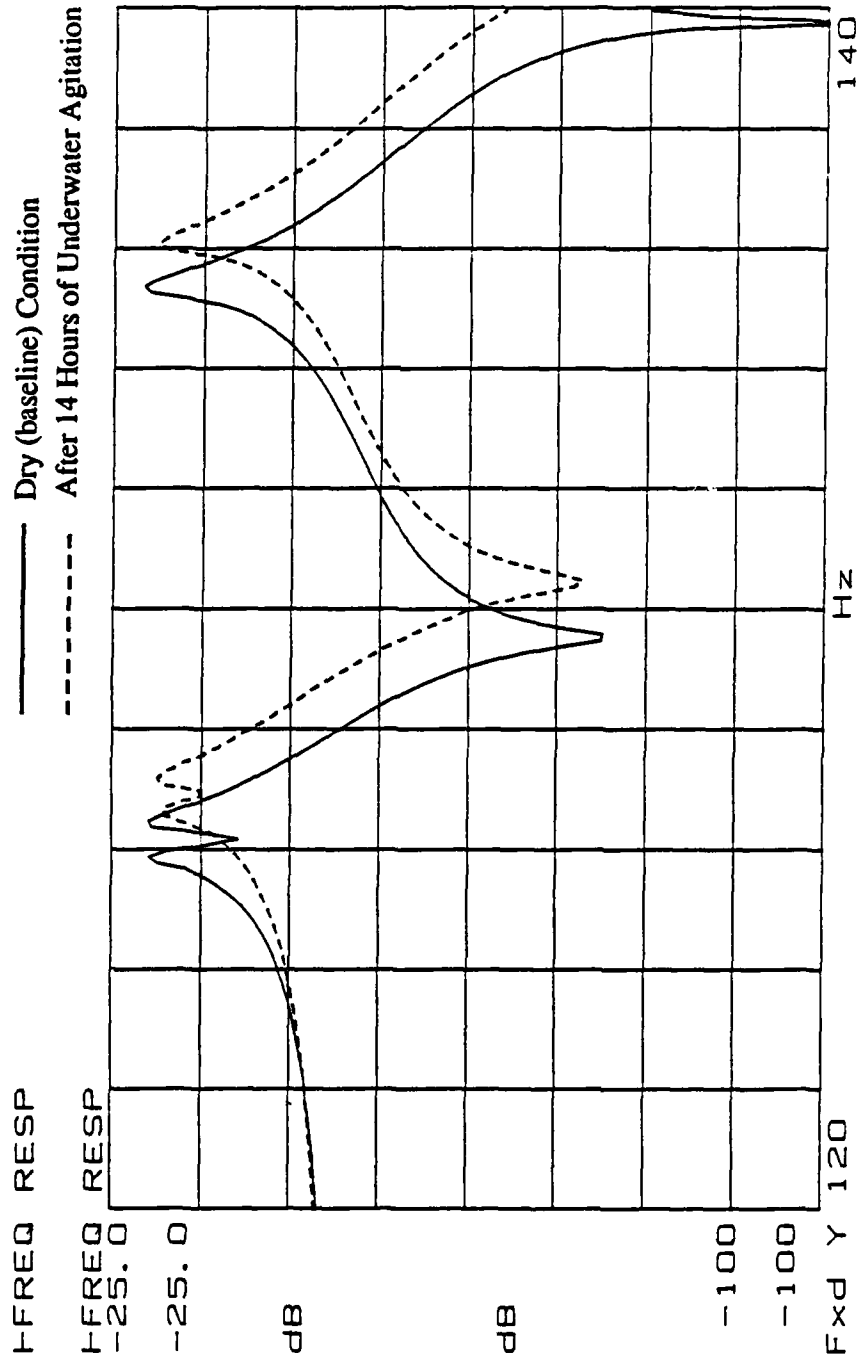

Figure 4.8. Frequency response of structure, measured on the shell, at 20 % bolt torque without viscoelastic material. Solid line represents the baseline condition and dashed line represents structure after 14 hours of underwater agitation.

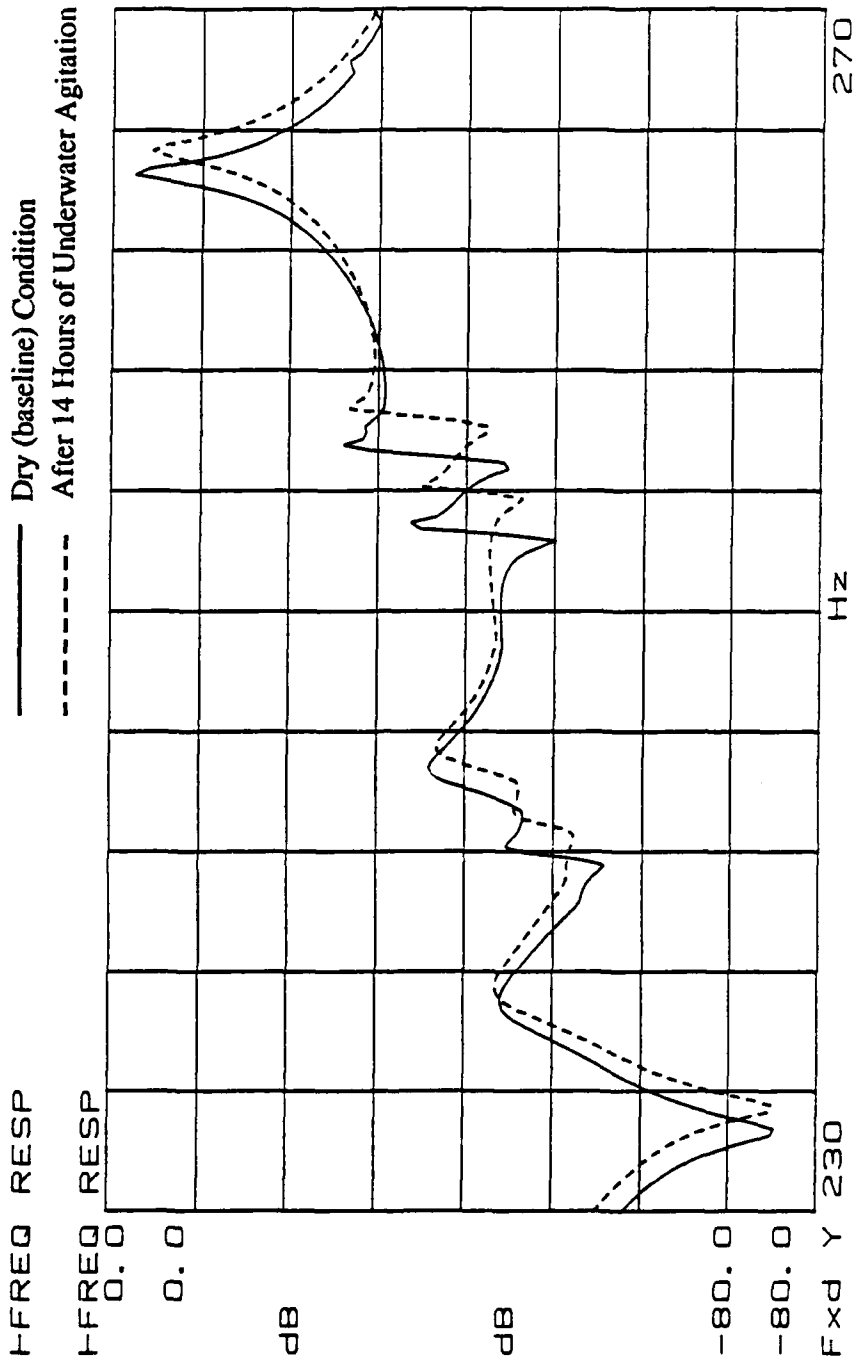

Figure 4.9. Frequency response of structure, measured on the shell, at 20 % bolt torque without viscoelastic material. Solid line represents the baseline condition and dashed line represents structure after 14 hours of underwater agitation.

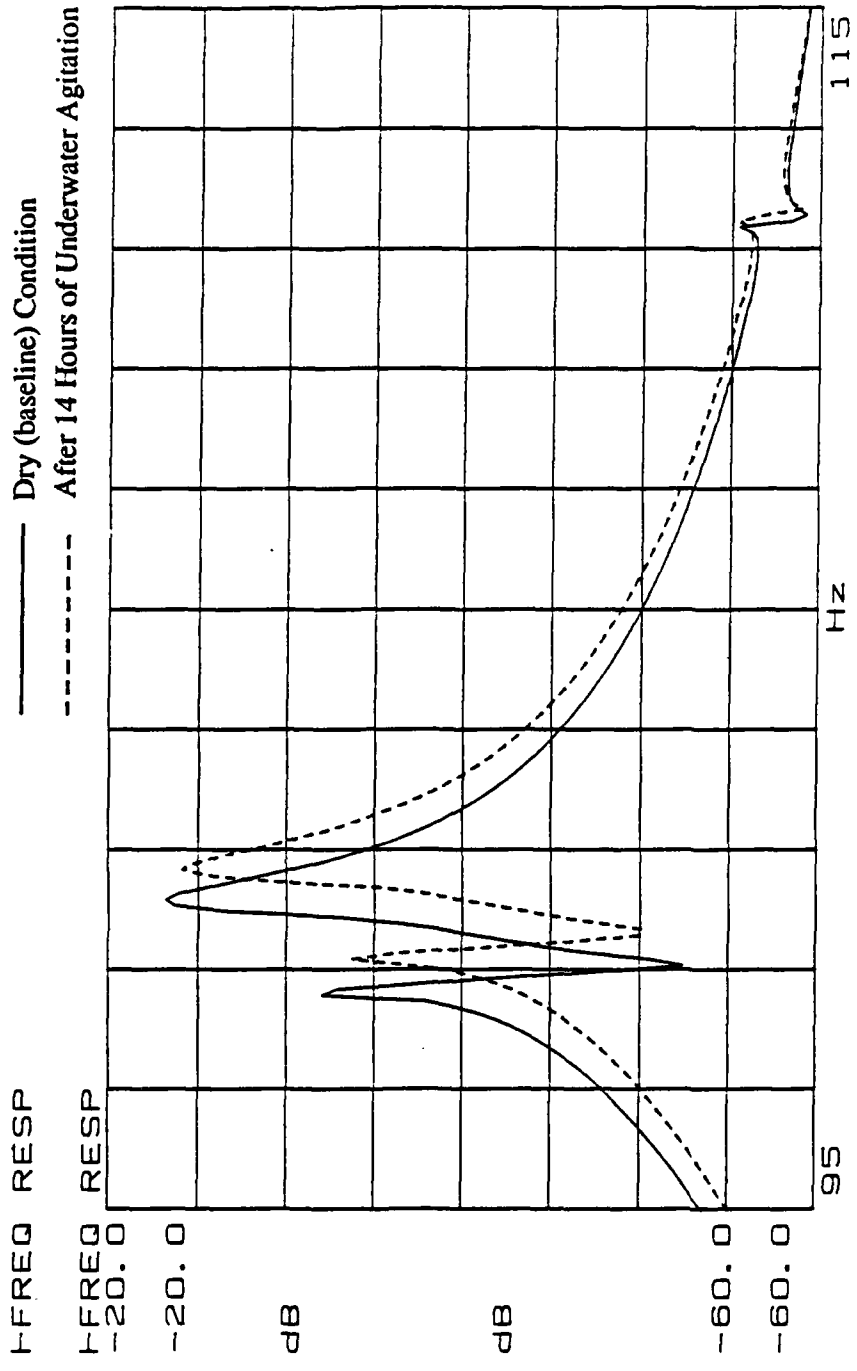

Figure 4.10. Frequency response of structure, measured on the vane, at 10 % bolt torque without viscoelastic material. Solid line represents the baseline condition and dashed line represents structure after 14 hours of underwater agitation.

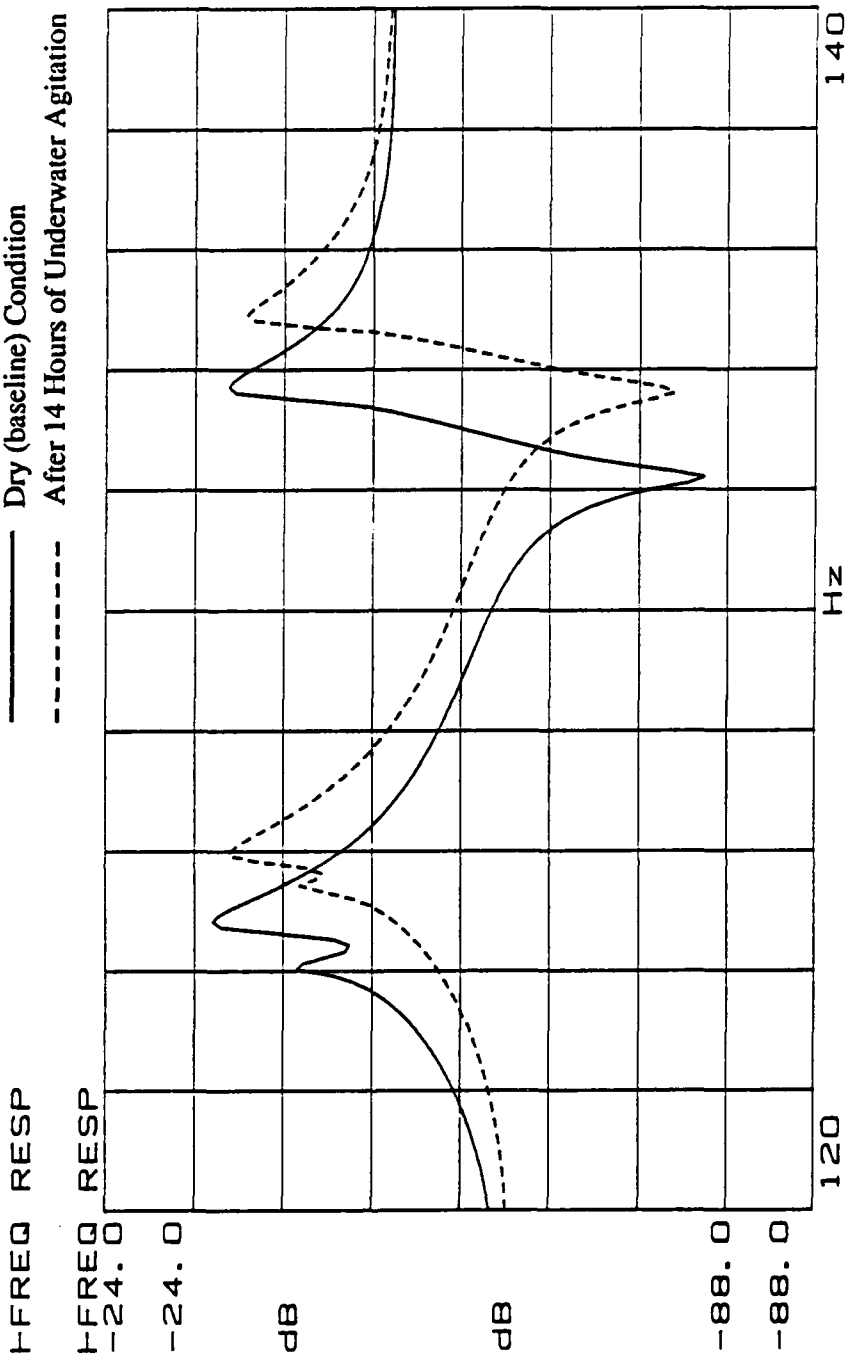

Figure 4.11. Frequency response of structure, measured on the vane, at 10 % bolt torque without viscoelastic material. Solid line represents the baseline condition and dashed line represents structure after 14 hours of underwater agitation.

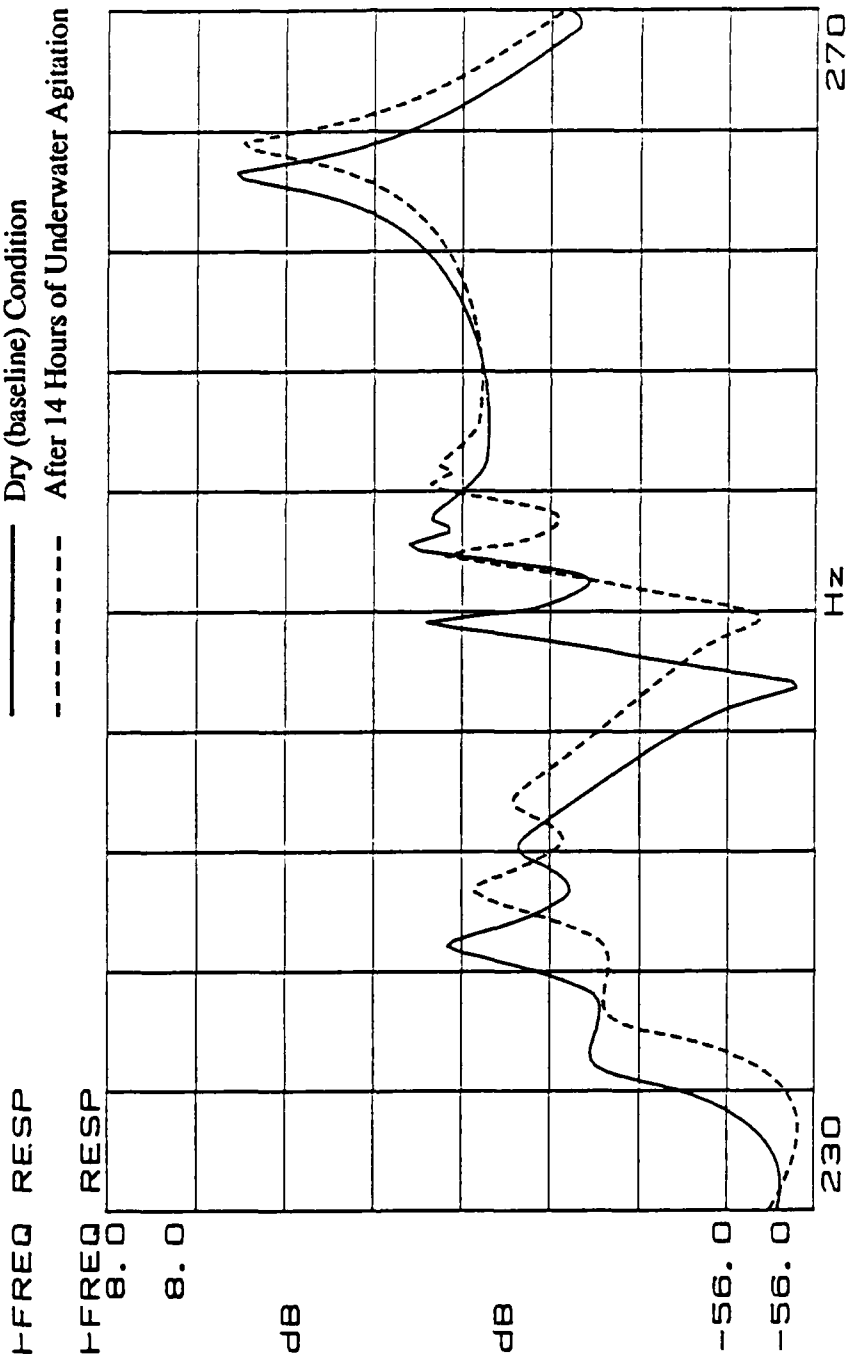

Figure 4.12. Frequency response of structure, measured on the vane, at 10 % bolt torque without viscoelastic material. Solid line represents the baseline condition and dashed line represents structure after 14 hours of underwater agitation.

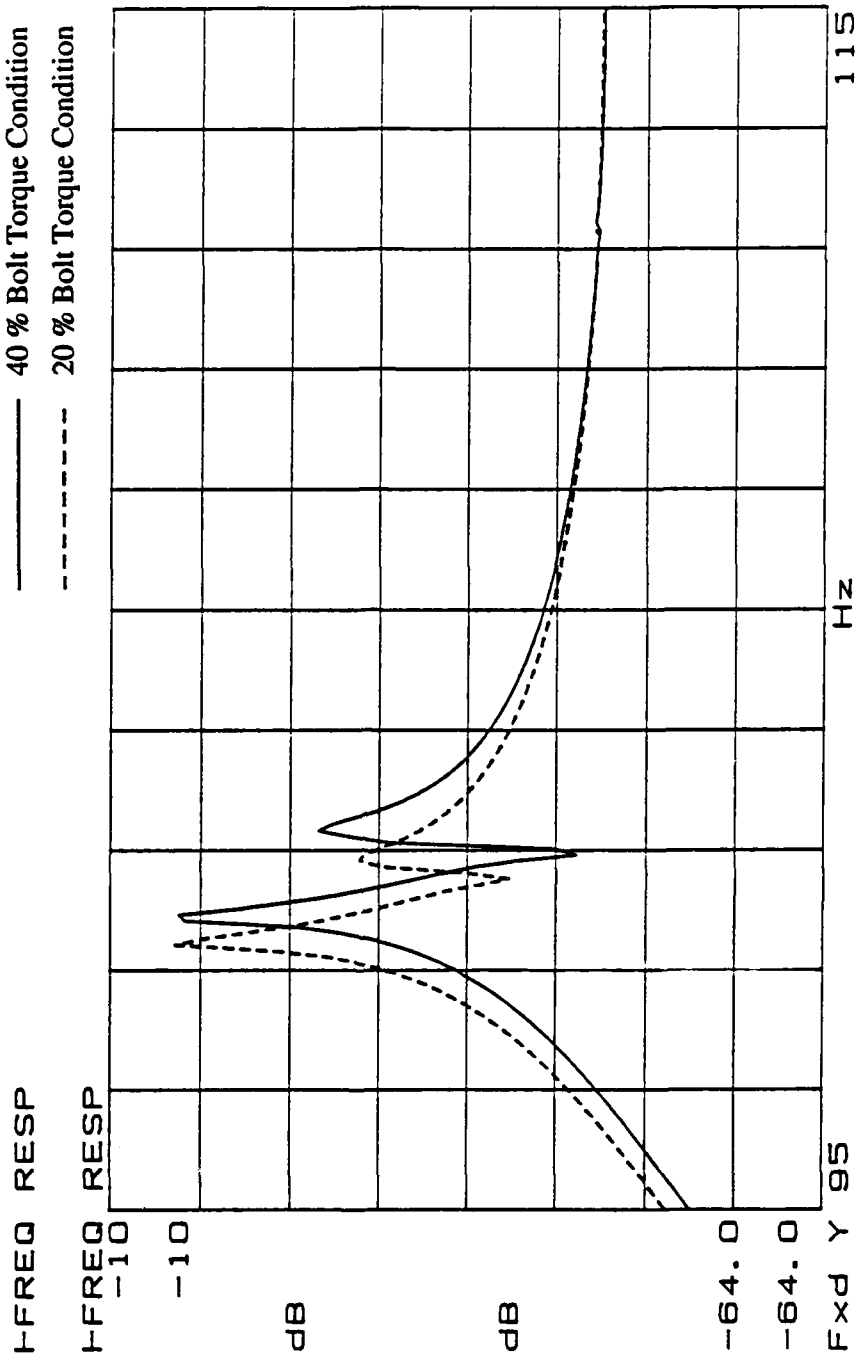

Figure 4.13. Frequency response of structure, measured on the shell, for two hours of underwater agitation. Solid line represents the 40 %bolt torque condition and the dashed line the 20 % bolt torque condition.

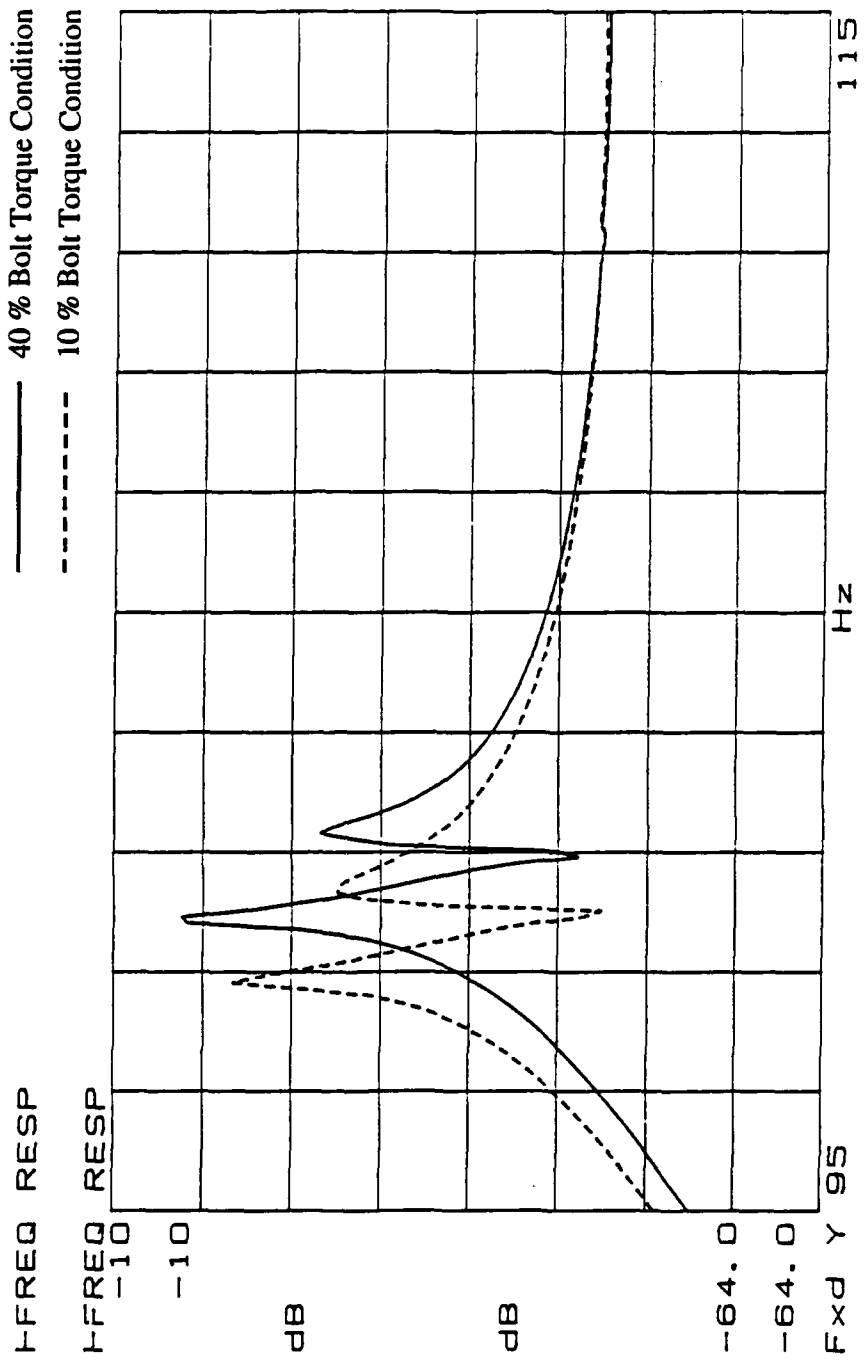

Figure 4.14. Frequency response of structure, measured on the shell, for two hours of underwater agitation. Solid line represents the 40 % bolt torque condition and the dashed line represents the 10 % bolt torque condition.

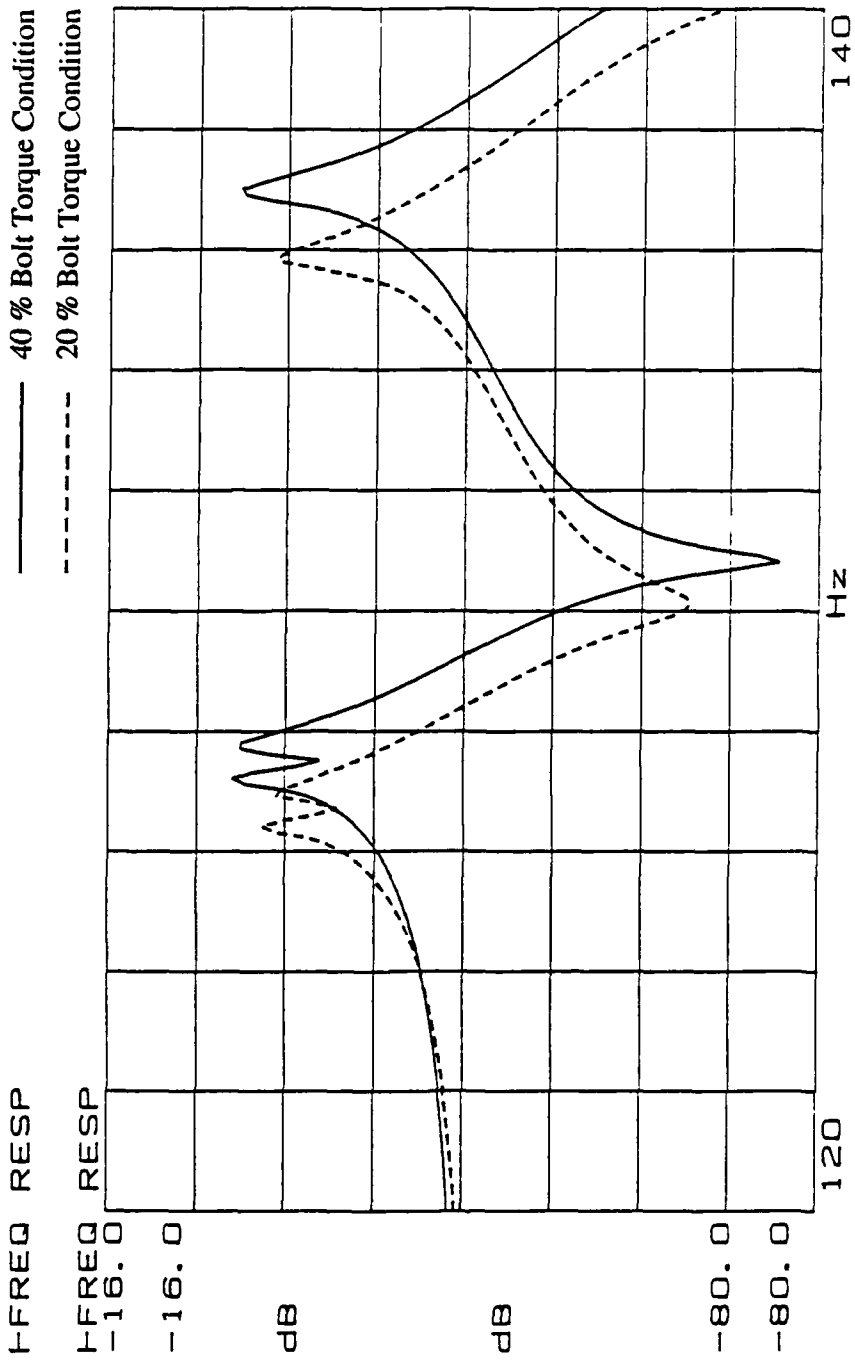

Figure 4.15. Frequency response of structure, measured on the shell, for two hours of underwater agitation. Solid line represents the 40 % bolt torque condition and the dashed line represents the 20 % bolt torque condition.

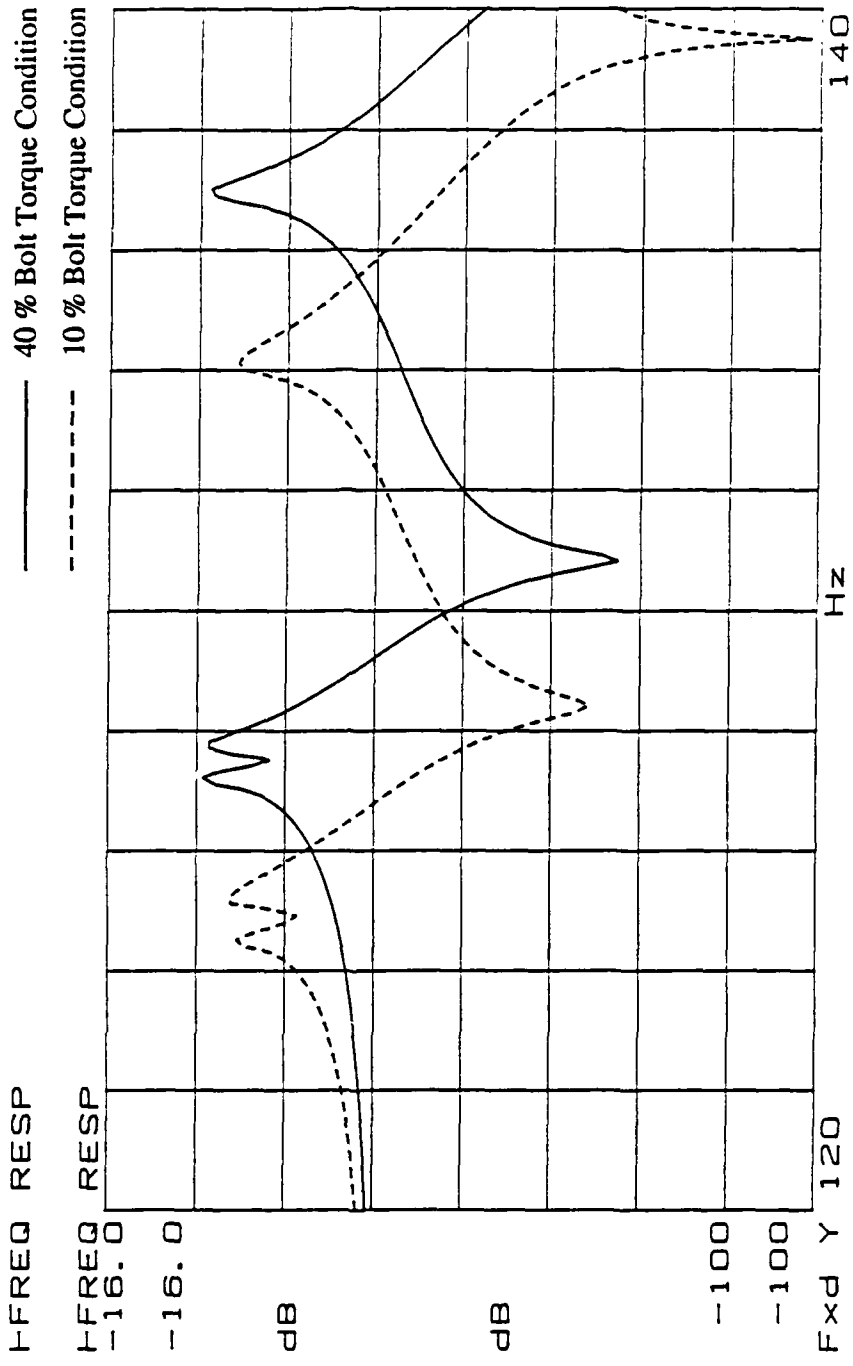

Figure 4.16. Frequency response of structure, measured on the shell, for two hours of underwater agitation. Solid line represents the 40 % bolt torque condition and the dashed line represents the 10 % bolt torque condition.

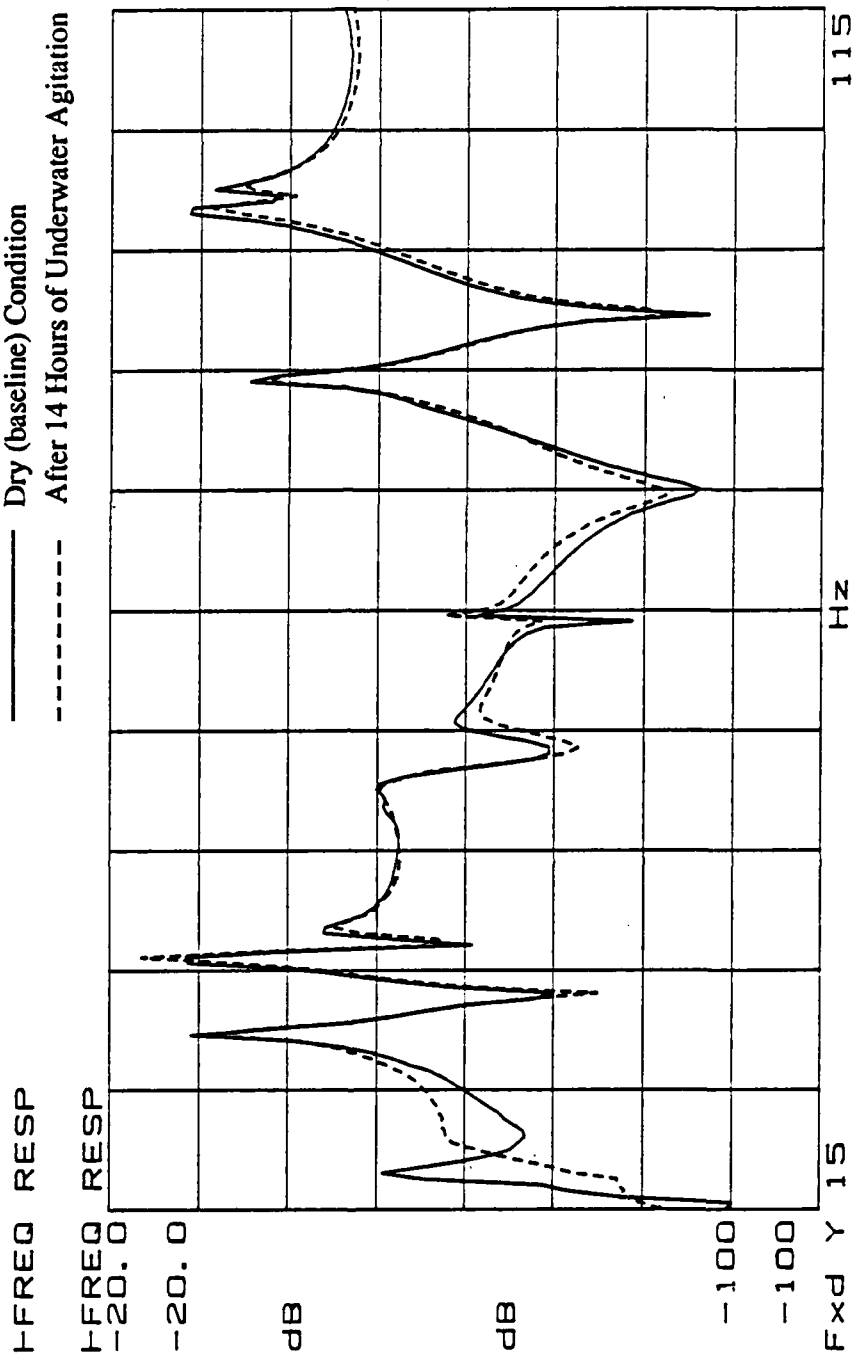

Figure 4.17. Frequency response of structure, measured on the shell, at 40 % bolt torque with viscoelastic material. Solid line represents the baseline condition and dashed line represents structure after 14 hours of underwater agitation.

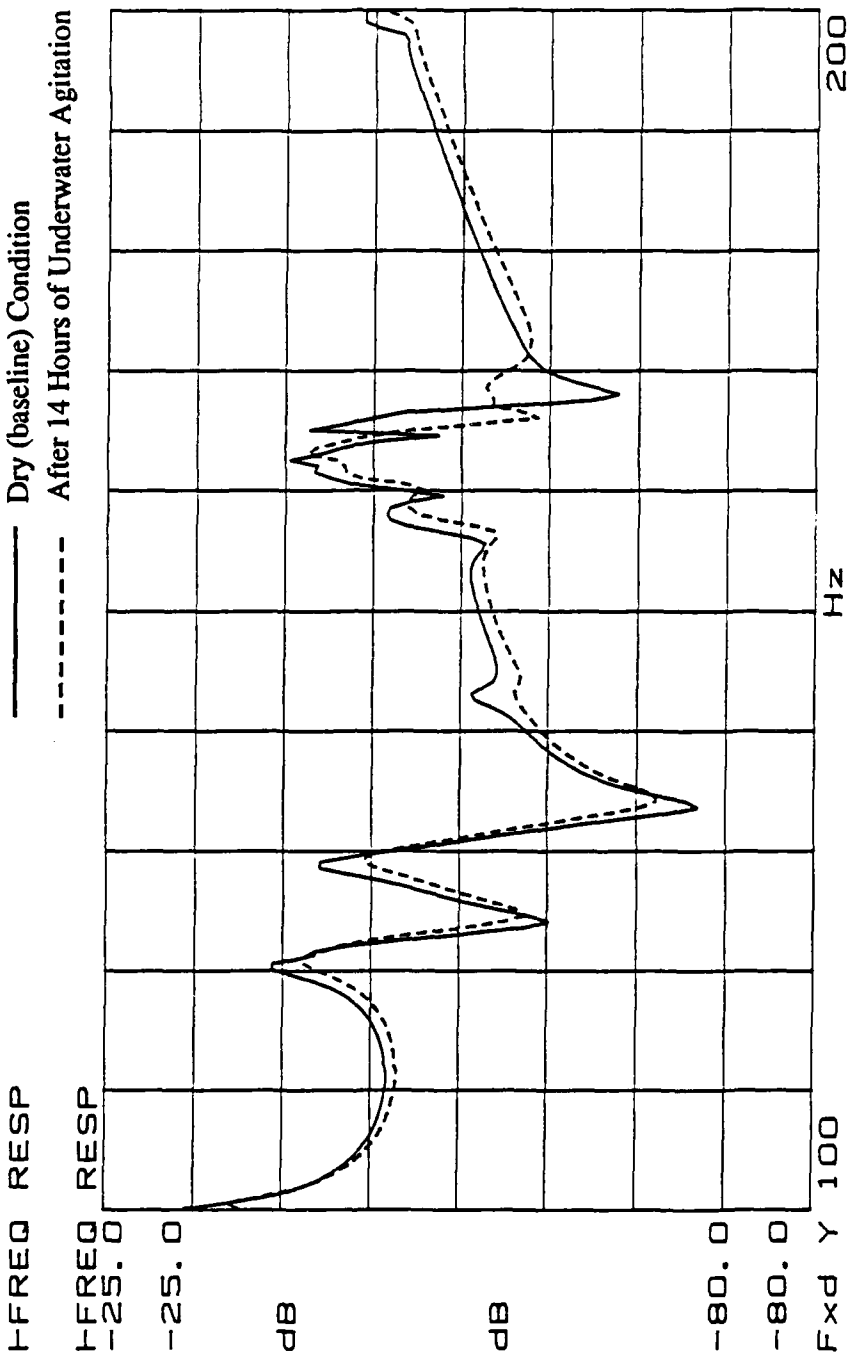

Figure 4.18. Frequency response of structure, measured on the shell, at 40 % bolt torque with viscoelastic material. Solid line represents the baseline condition and dashed line represents structure after 14 hours of underwater agitation.

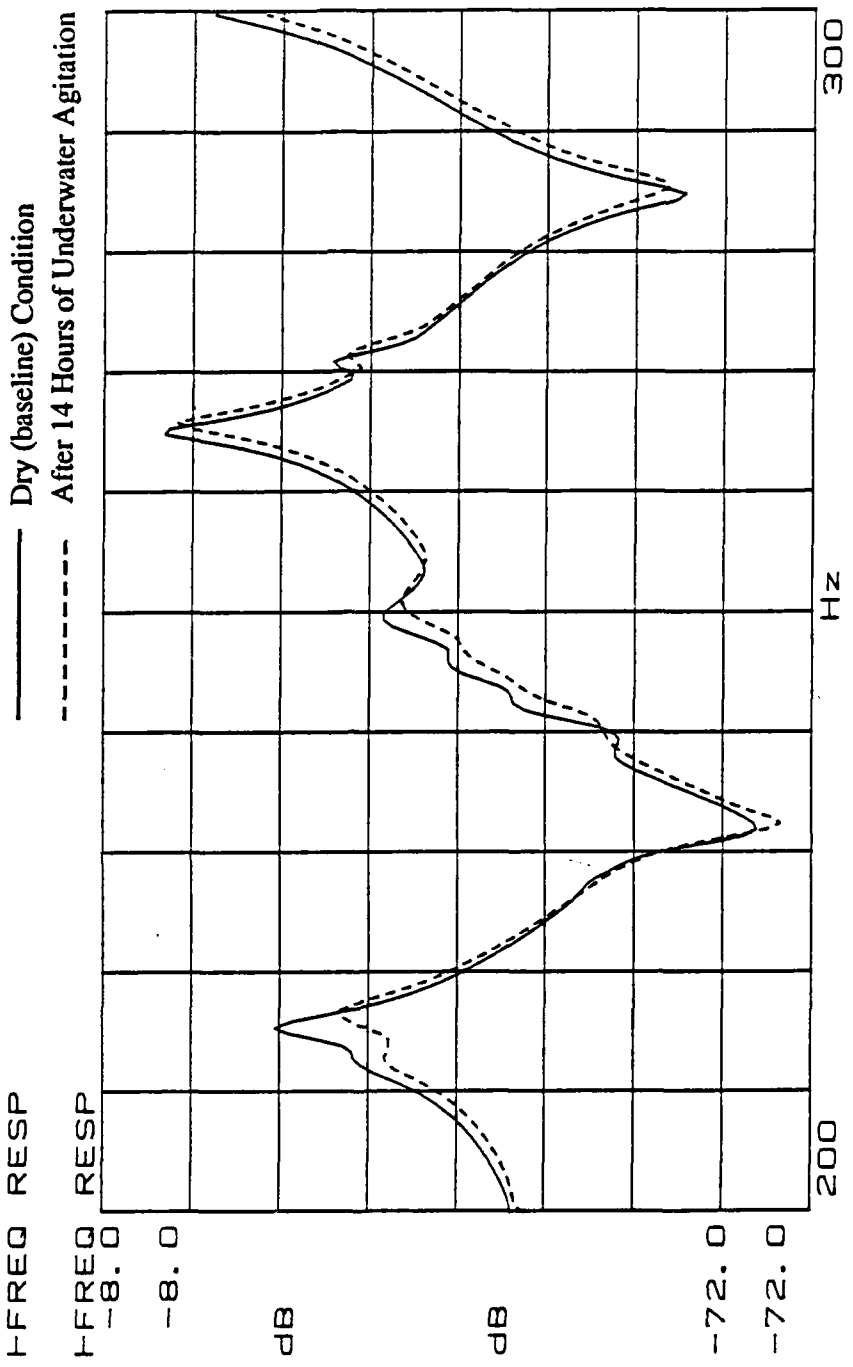

Figure 4.19. Frequency response of the structure, measured on the shell, at 40 % bolt torque with viscoelastic material. Solid line represents the baseline condition and the dashed line represents the structure after 14 hours of underwater agitation.

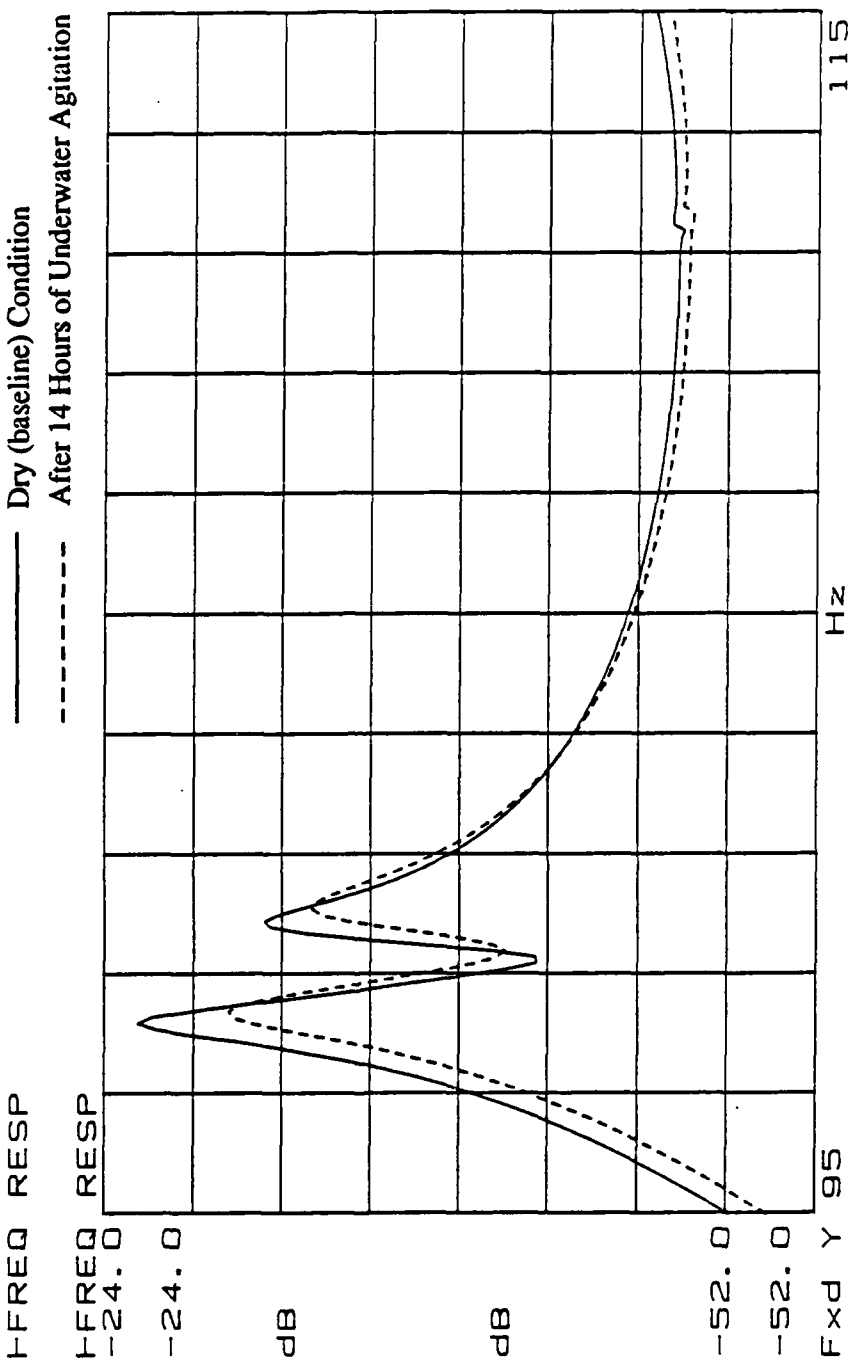

Figure 4.20. Frequency response of the structure, measured on the shell, at 40 % bolt torque with viscoelastic material. The solid line represents the baseline condition and the dashed line represents the structure after 14 hours of underwater agitation.

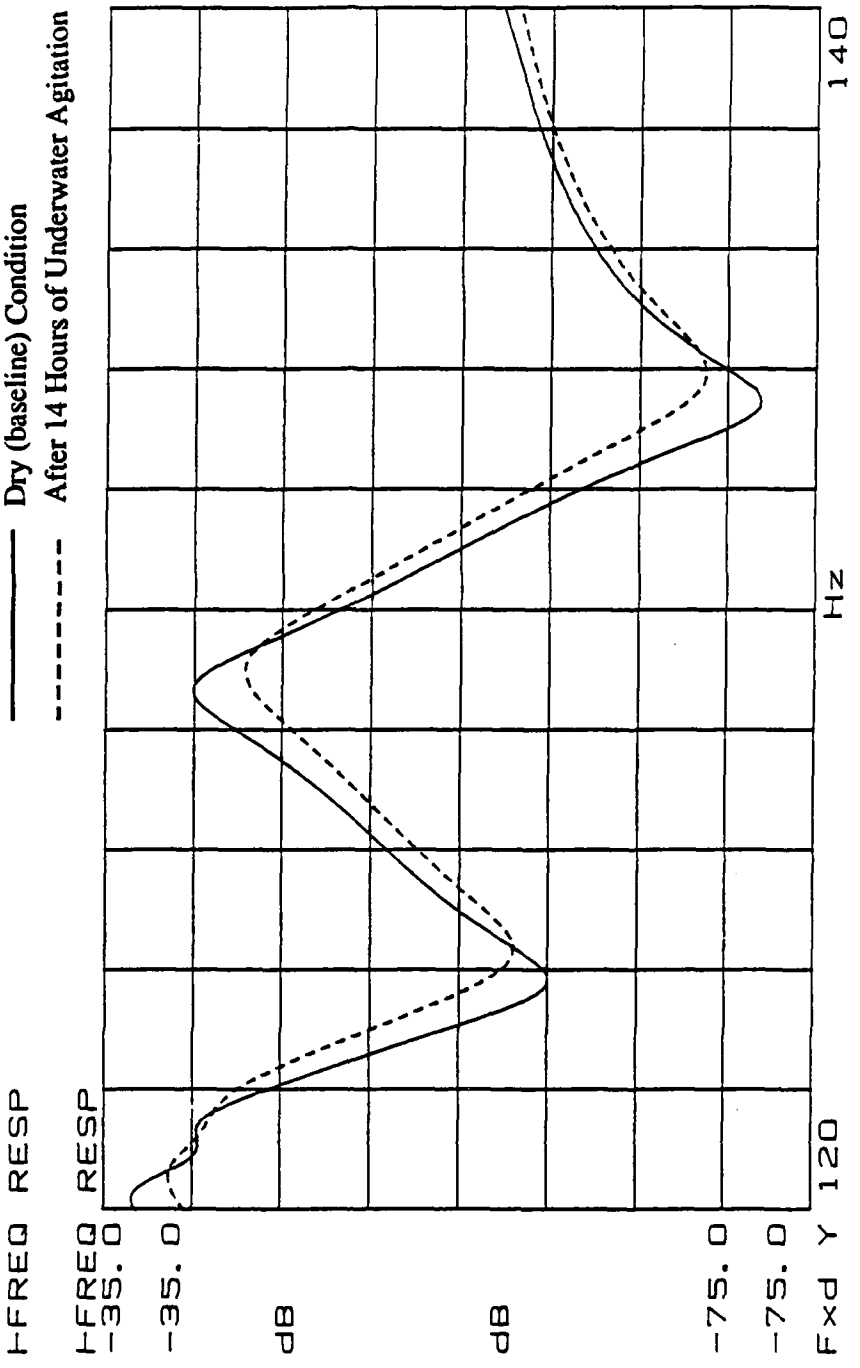

Figure 4.21. Frequency response of the structure, measure on the shell, at 40 % bolt torque with viscoelastic material. Solid line represents the baseline condition and the dashed line represents the structure after 14 hours of underwater agitation.

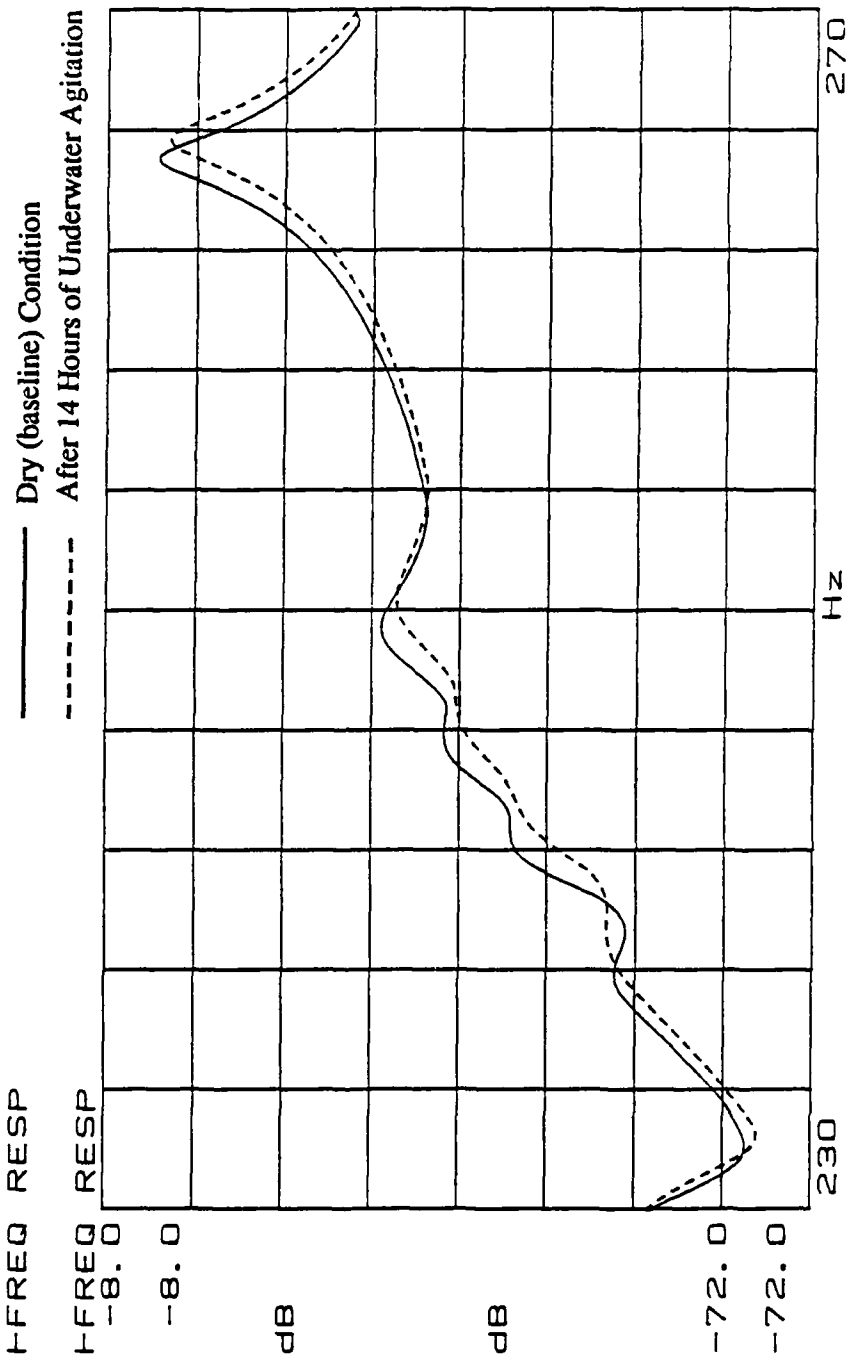

Figure 4.22. Frequency response of the structure, measured on the shell, at 40 % bolt torque with viscoelastic material. The solid line represents the baseline condition and the dashed line represents the structure after 14 hours of underwater agitation.

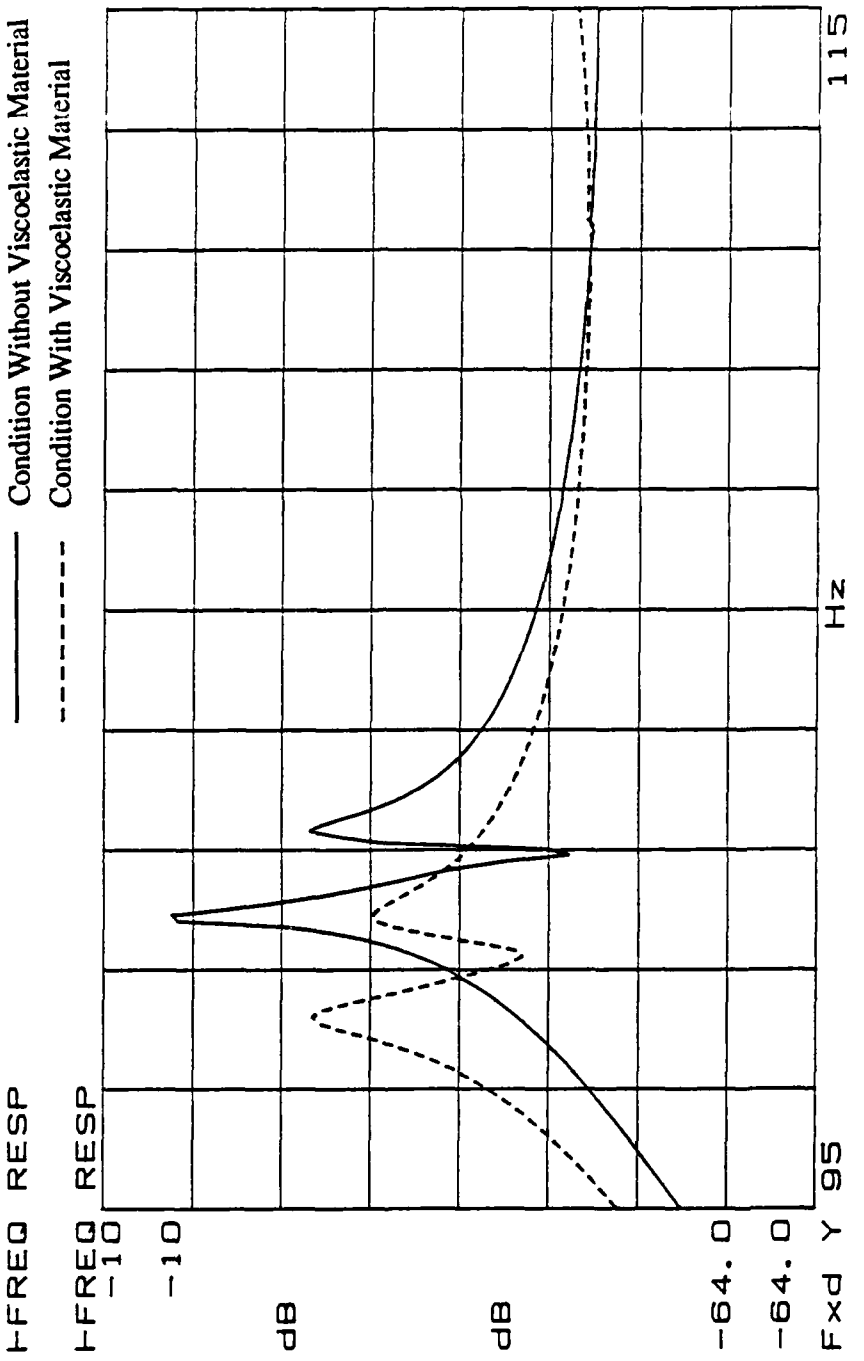

Figure 4.23. Frequency response of the structure, measured on the shell, for two hours of underwater agitation and 40 % bolt torque. The solid line represents the condition without viscoelastic material and the dashed line represents the condition with viscoelastic material.

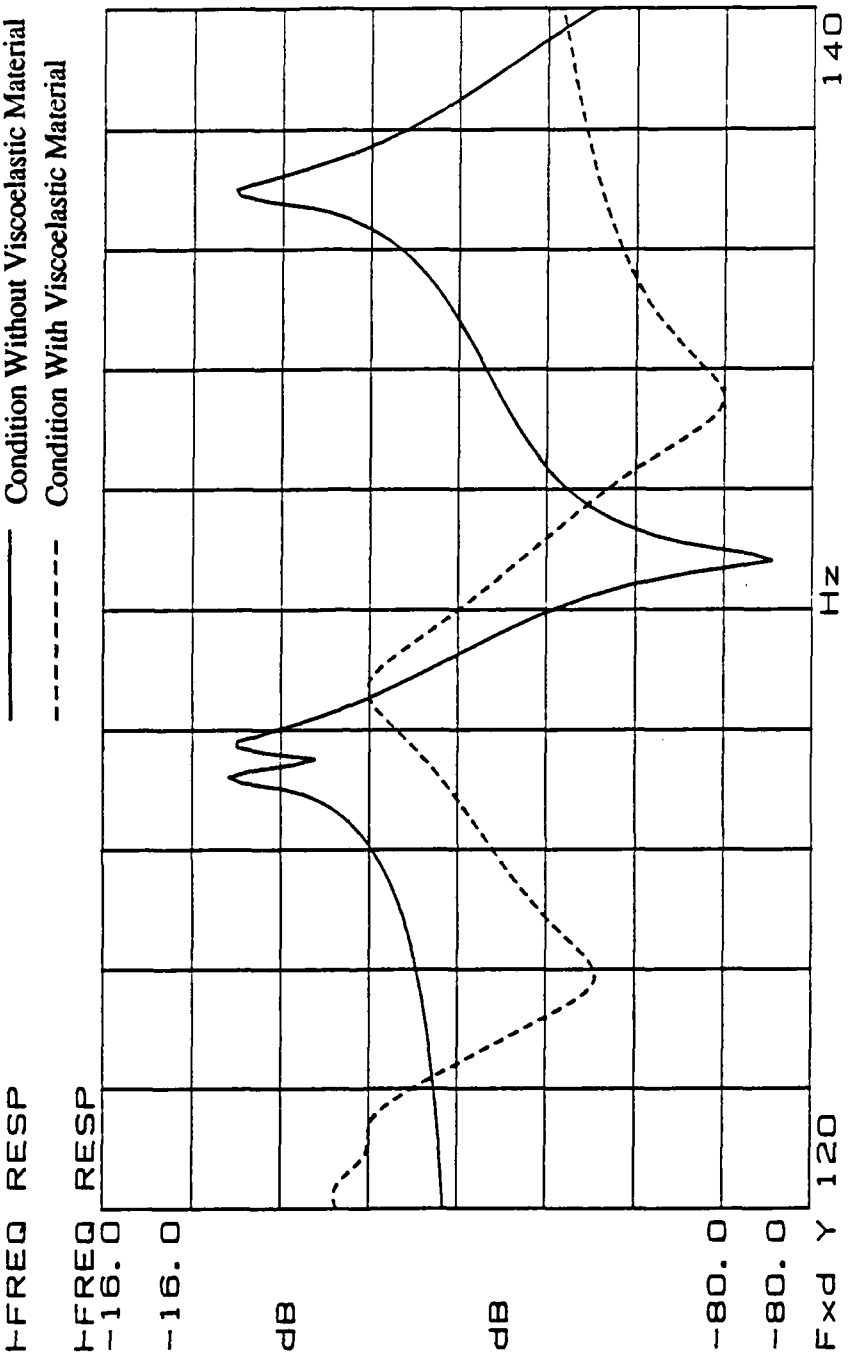

Figure 4.24. Frequency response of the structure at 40 % bolt torque, measure on the shell, for two hours of underwater agitation. The solid line represents the condition without viscoelastic material and the dashed line represents the condition with viscoelastic material.

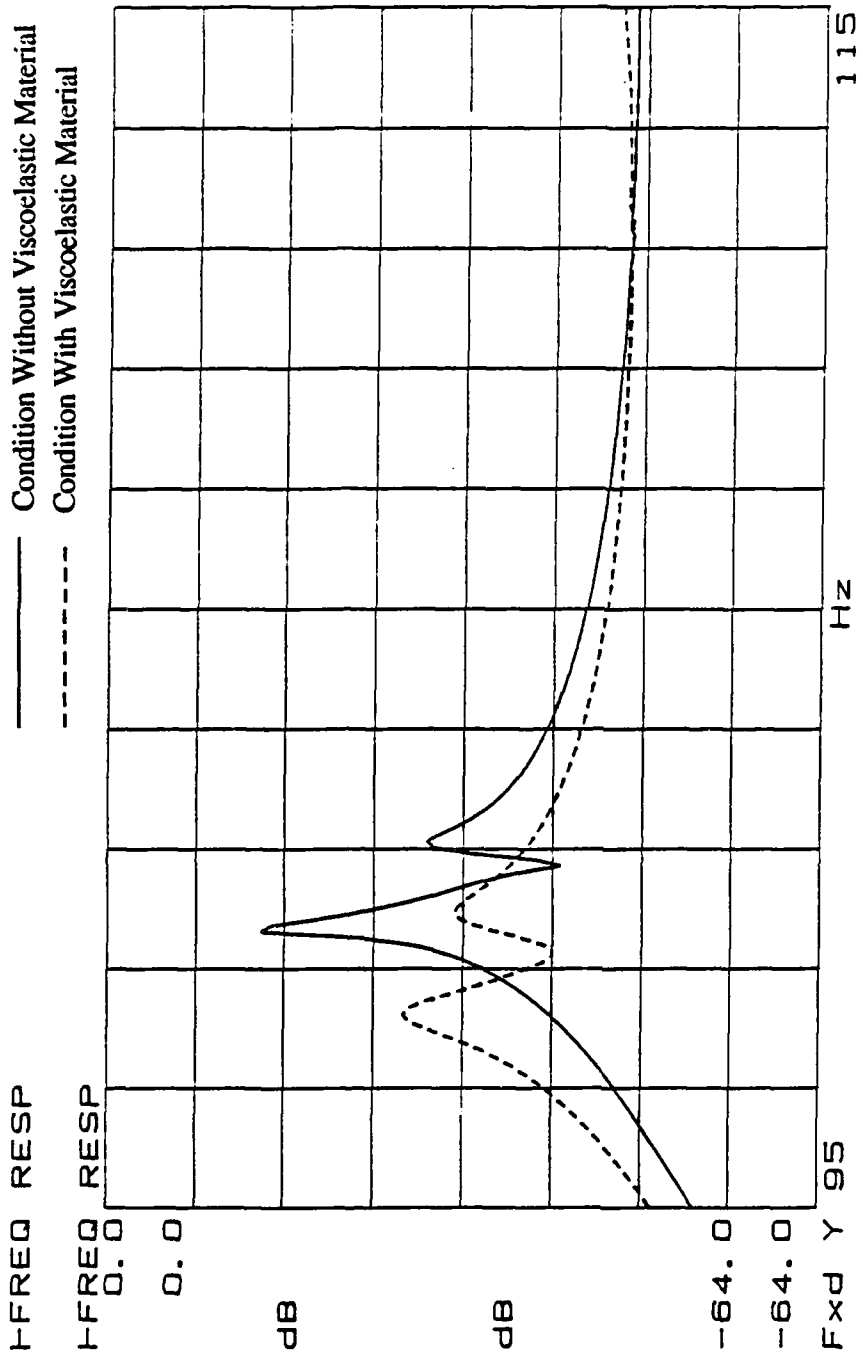

Figure 4.25 Frequency response of the structure, measured on the shell, after maximum underwater agitation time at 20 % bolt torque. The solid line represents the condition without viscoelastic material and the dashed line represents the condition with viscoelastic material.

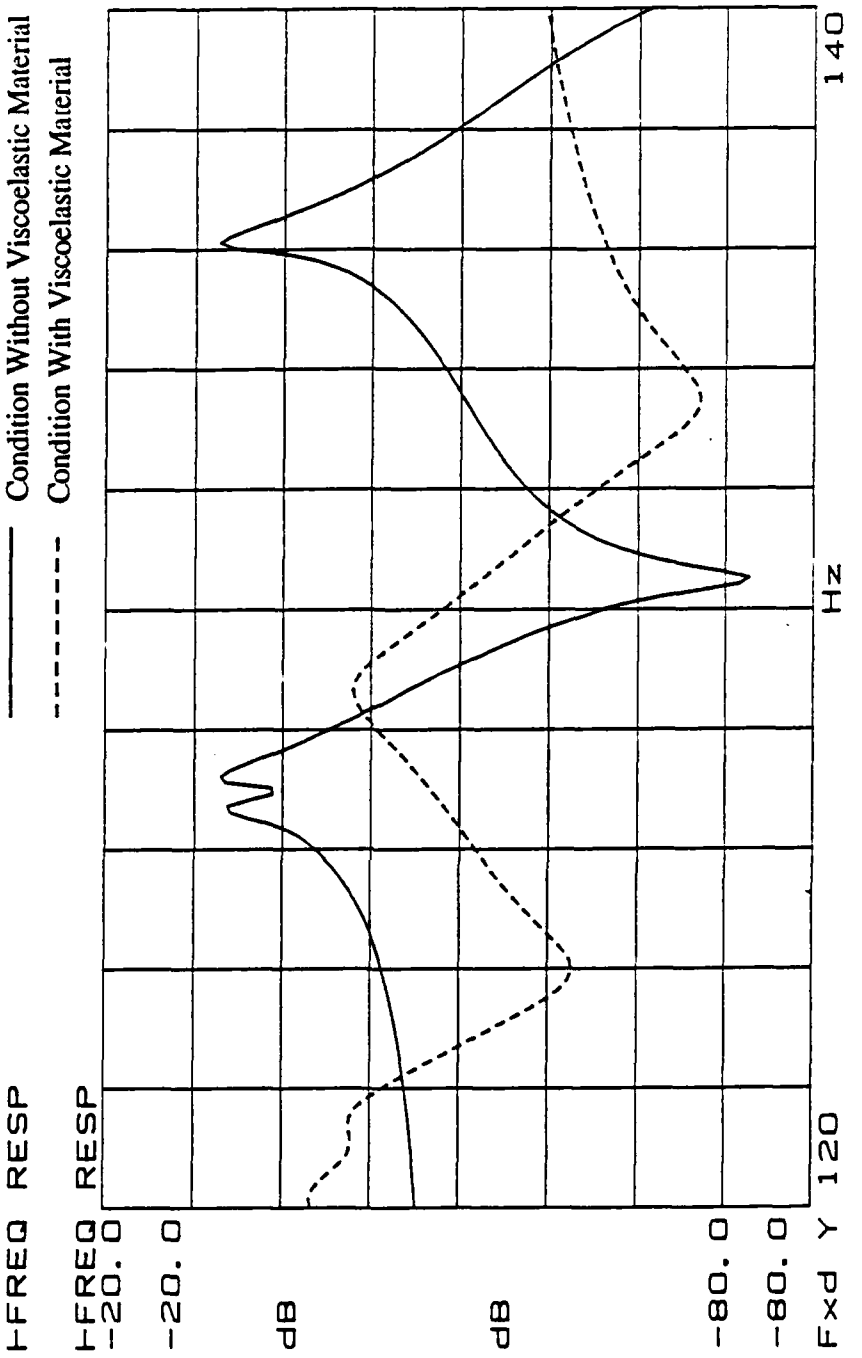

Figure 4.26 Frequency response of the structure, measured on the shell, after maximum underwater agitation time at 20 % bolt torque. The solid line represents the condition without viscoelastic material and the dashed line represents the condition with viscoelastic material.

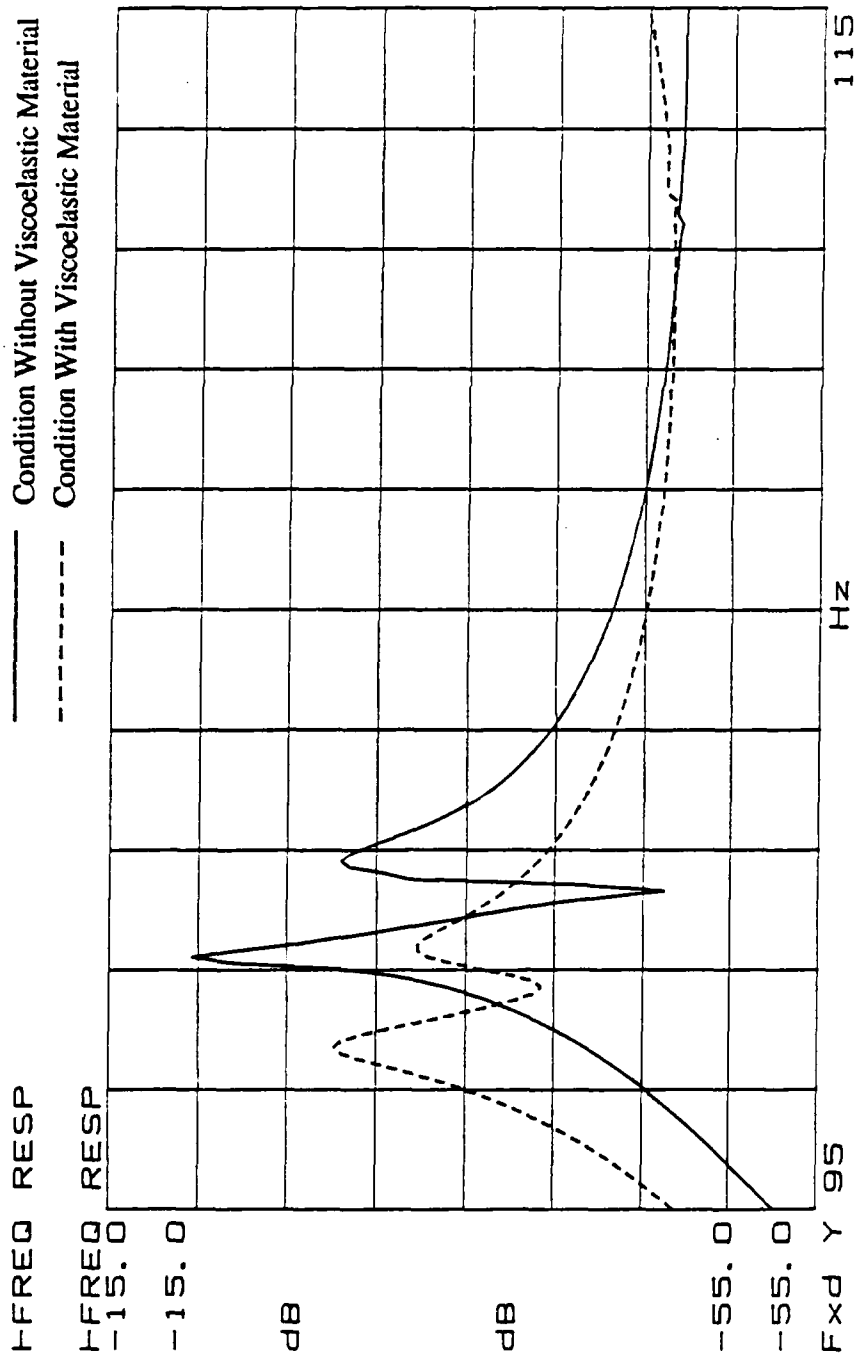

Figure 4.27 Frequency response of the structure, measured on the shell, after maximum underwater agitation time at 10 % bolt torque. The solid line represents the condition without viscoelastic material and the dashed line represents the condition with viscoelastic material.

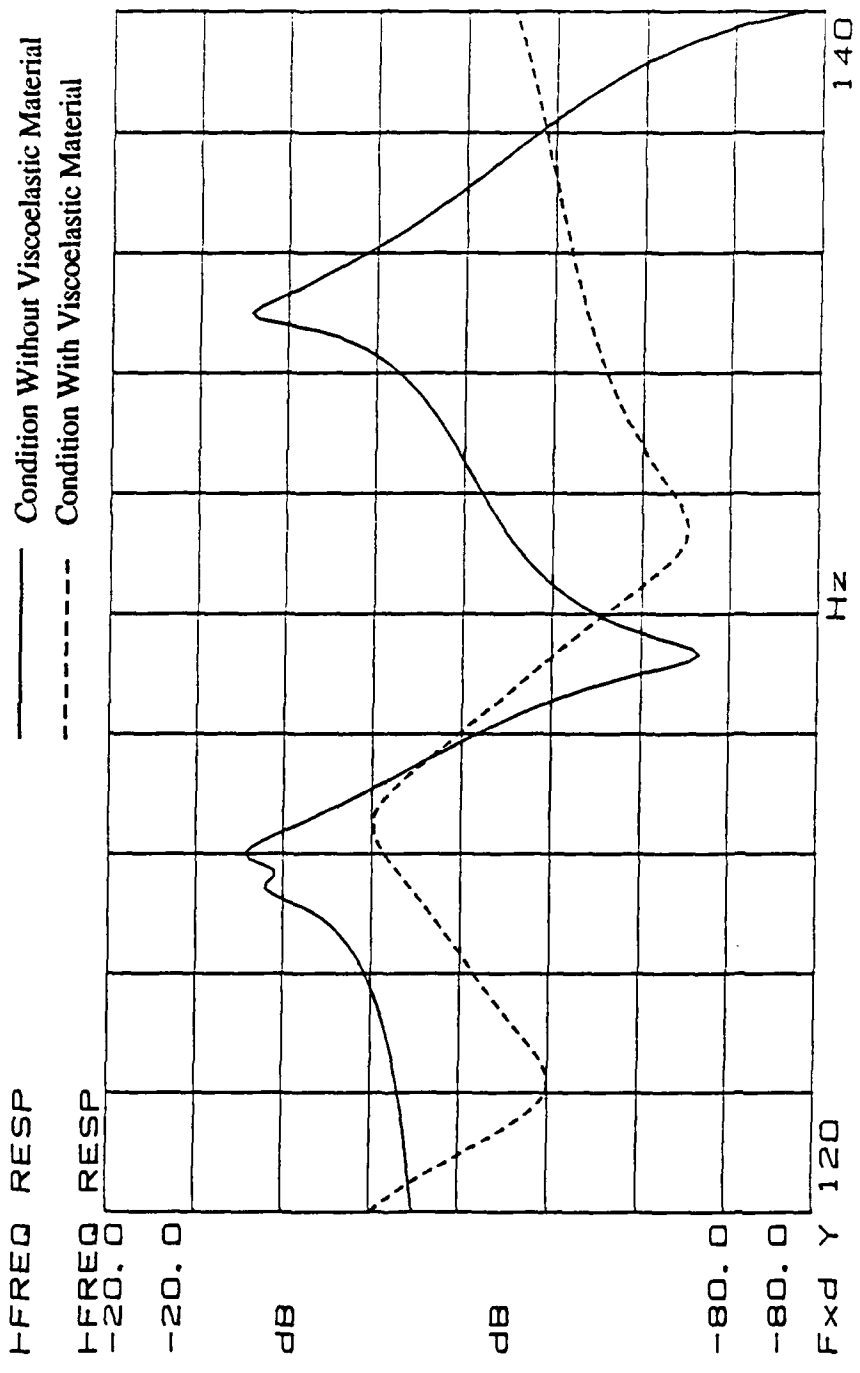

Figure 4.28 Frequency response of the structure, measured on the shell, after maximum underwater agitation time at 10 % bolt torque. The solid line represents the condition without viscoelastic material and the dashed line represents the condition with viscoelastic material.

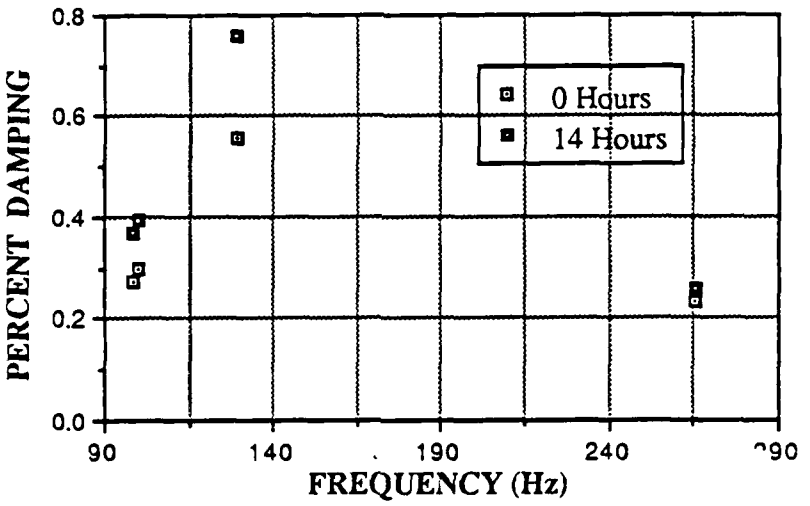

Figure 4.29 Percent damping for structure with 40 % bolt torque with viscoelastic material applied at the joint interface.

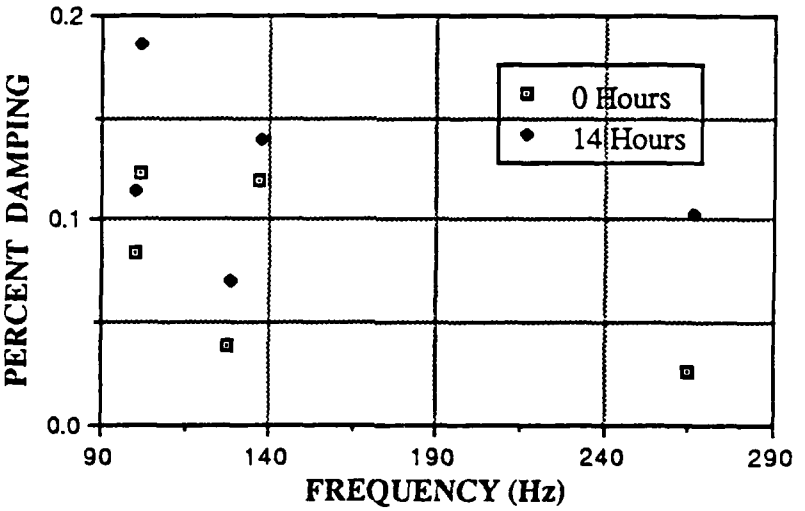

Figure 4.30 Percent damping for structure with 40 % bolt torque with no viscoelastic material.

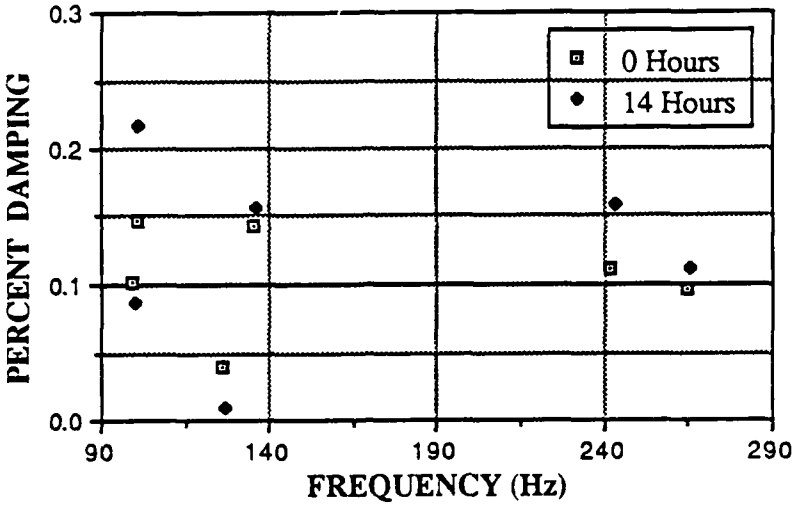

Figure 4.31 Percent damping for structure with 20 % bolt torque and no viscoelastic material.

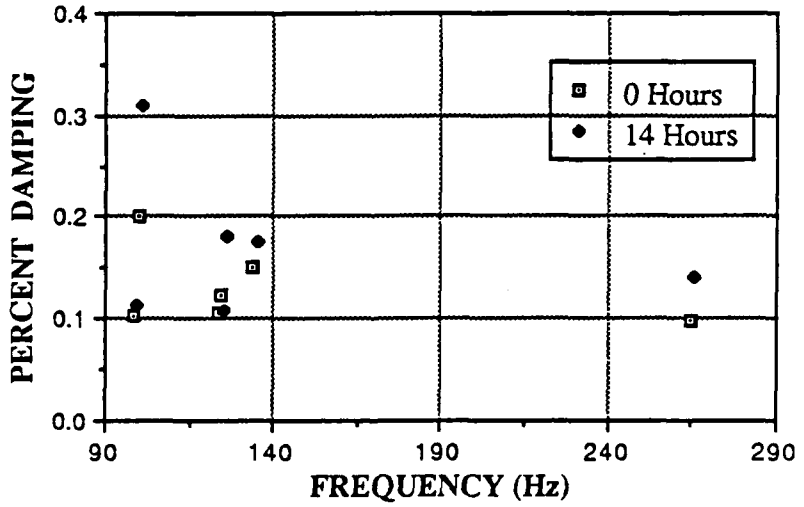

Figure 4.32 Percent damping for structure with 10 % bolt torque and no viscoelastic material.

V. CONCLUSIONS

Following Iverson's [Ref. 1] investigation of the damping characteristics of the bolted structure, there was concern about how the bolted structure would perform in an underwater environment. It was thought that the water could act as a lubricant, causing increased microslip or even causing the joint interfaces to pass from the microslip region into the macroslip region, which would have resulted in reduced structural stiffness. This did not occur and instead structural stiffness increased, as evidenced by the upward shift of the frequency response functions. Structural damping also increased following the underwater agitation.

The increase in structural stiffness and damping is a direct result of water replacing air at the joint interfaces during the underwater agitation. As was previously discussed in this paper, a system with a thin viscous fluid layer between two plates acted upon by a harmonic force will exhibit viscous fluid damping. Imperfect mating of the plate surfaces at the joint interfaces allowed air to remain between the plates after the structure was assembled. Prior to the underwater agitation, the viscous fluid between the plates of the structure under investigation was air. As the structure was agitated underwater over time, water gradually replaced the air between the plates at the joint interfaces. The increased density and viscosity of the water resulted in increased structural stiffness and damping as predicted by the equations of Ingard and Akay [Ref 7]. Eventually the water completely replaced the air at the joint interfaces and the stiffness and damping no longer changed with increasing underwater agitation time.

Summarizing, reduced bolt torque and the use of viscoelastic material at the joint interface shifted the frequency response down while the effects of underwater agitation resulted in an upward frequency shift. All three effects resulted in increased damping and a decrease in the frequency response amplitudes.

The application of the viscoelastic material at the joint interfaces is effective in reducing system response in both a dry or wet environment. However, the relatively low system damping, even with the addition of the damping material, suggests that further damping treatments are in order.

VI. RECOMMENDATIONS

The plate and shell structure in this investigation was complex and it was therefore difficult to separate the interactions of the various effects upon the structure. The study of a simpler structure might more easily allow the separation and study of the complex interactions of the various effects. The effects of any lubrication that might have occured due to the presence of water at the joint could not be noted in this study but might be identified in the study of a simpler structure.

The highest damping for any mode of the structure noted under any condition was less than one percent. The damping material was placed at the bolted joint interfaces out of convenience without taking into account the mode shapes of the structure or the frequencies of interest. The placement of constrained layer treatments based on the mode shapes of the structures and frequencies of interest, to maximize the structural damping, should be investigated.

LIST OF REFERENCES

1. Iverson, J. C., Experimental Investigation of Damping Characteristics of Bolted Structural Connections for Plates and Shells M. S. and Mechanical Engineer Thesis, Naval Postgraduate School, Monterey, California, September 1987.

2. Beards, C. F., and Woowat, A., "The Control of Frame Vibration by Friction Damping in Joints," J. of Vibration, Acous., Stress, and Reliability in Design, Vol. 107, January 1985, pp. 26-32.

3. Nelson, F. C., and Sullivan, D. F., "Damping in Joints of Built-Up Structures," Proceedings-Institute of Environmental Sciences, Twenty Second, 1976, pp. 87-90.

4. Ramsey, K. A., "Effective Measurements for Structural Dynamics Testing," Sound and Vibration, November 1975, pp. 24-35.

5. Hewlett-Packard Company, The Fundamentals of Modal Testing, Application Note 243-3.

6. Nashif, A. D., Jones, D. I. G., Henderson, J. P., Vibration Damping, Wiley, New York, 1985, pp. 67-68, 89-94, 278-294.

7. Ingard, K. U., Akay, A., "On the Vibration of a Plate by Means of a Viscous Fluid Layer," Transactions of the ASME, Vol. 109, April 1987, pp. 178-184.

INITIAL DISTRIBUTION LIST

1.	Defense Technical Information Center Cameron Station Alexandria, Virginia 22304-6145	2
2.	Library, Code 0142 Naval Postgraduate School Monterey, California 93943-5002	2
3.	Dean of Science and Engineering, Code 06 Naval Postgraduate School Monterey, California 93943-5000	2
4.	Research Administration Office, Code 012 Naval Postgraduate School Monterey, California 93943-5000	1
5.	Department Chairman, Code 69 Department of Mechanical Engineering Naval Postgraduate School Monterey, California 93943-5000	1
6.	Professor Y. S. Shin, Code 69Sg Department of Mechanical Engineering Naval Postgraduate School Monterey, California 93943-5000	3
7.	Dr. K. Kim, Code 69Ki Department of Mechanical Engineering Naval Postgraduate School Monterey, California 93943-5000	1
8.	Dr. Arthur Kilcullen, Code 1962 David W. Taylor Naval Ship R&D Center Annapolis, Maryland 21402	5
9.	Dr. Lawrence Maga, Code 1962 David W. Taylor Naval Ship R&D Center Annapolis, Maryland 21402	1
10.	Mr. Robert Hardy, Code 2803 David W. Taylor Naval Ship R&D Center Annapolis, Maryland 21402	1
11.	Mr. V. J. Castelli, Code 2844 David W. Taylor Naval Ship R&D Center Annapolis, Maryland 21402	1

12. Dr. D. J. Vendittis, Code 196 — 1
David W. Taylor Naval Ship R&D Center
Ship Acoustics Department (196)
Bethesda, Maryland 20084

13. Dr. B. Whang, Code 1750.2 — 1
David W. Taylor Naval Ship R&D Center
Hull Group Head, Submarine Protection Div.
Bethesda, Maryland 20084

14. Dr. N. T. Tsai — 1
Defense Nuclear Agency
SSPS
Washington, D.C. 20305-1000

END

DATE

FILMED

8-88

DTIC